Article

In situ identification of both IL-4 and IL-10 Cytokine-Receptor Interactions during tissue regeneration

Krisztina Nikovics *, Anne-Laure Favier, Mathilde Rocher, Céline Mayinga, Johanna Gomez, Frédérique Dufour-Gaume, Diane Riccobono

Posted Date: 23 April 2023

doi: 10.20944/preprints202304.0741.v1

Keywords: IL-4; IL-10; receptor; interaction; regeneration; Proximity ligation assay

Article

In Situ Identification of Both IL-4 and IL-10 Cytokine-Receptor Interactions during Tissue Regeneration

Krisztina Nikovics [1,*], Anne-Laure Favier [1], Mathilde Rocher [1], Céline Mayinga [1], Johanna Gomez [1], Dufour-Gaume Frédérique [2] and Diane Riccobono [3]

[1] Imagery Unit, Department of Platforms and Technology Research, French Armed Forces Biomedical Research Institute, 91223 Brétigny-sur-Orge, France; anne-laure.favier@intradef.gouv.fr (A.-L.F.); mrocher989@gmail.com (M.R.); celine.mayinga@supbiotech.fr (C.M.); johanna.gomes@supbiotech.fr (J.G)

[2] War Traumatology Unit, Department of NRBC Defense; French Armed Forces Biomedical Research Institute, 91223 Brétigny-sur-Orge, France; frederique.dufour-gaume@def.gouv.fr

[3] Radiobiology Unit, Department of NRBC Defense; French Armed Forces Biomedical Research Institute, 1, place du Général Valérie André, BP73, 91223 Brétigny-sur-Orge, France. diane.riccobono@intradef.gouv.fr

* Correspondence: krisztina.nikovics@def.gouv.fr or krisztina.nikovics@intradef.gouv.fr; Tel.: +33-(0)-1-78-65-13-331

Abstract: Cytokines secreted by individual immune cells regulate tissue regeneration and allow communication between various cell types. Cytokines bind to cognate receptors and trigger the healing process. Determining the orchestration of cytokine interactions with their receptors on their cellular targets is essential to fully understand the process of inflammation and tissue regeneration. To this end, we have investigated the interactions of Interleukin-4 cytokine (IL-4)/Interleukin-4 cytokine receptor (IL-4R) and Interleukin-10 cytokine (IL-10)/Interleukin-10 cytokine receptor (IL-10R) using *in situ* Proximity Ligation Assays in a regenerative model of skin, muscle and lung tissues in the mini-pig. The pattern of protein-protein interactions was distinct for the two cytokines. IL-4 bound predominantly to receptors on macrophages and endothelial cells around the blood vessels while the target cells of IL-10 were mainly receptors on muscle cells. Our results show that *in situ* studies of cytokine-receptor interactions can provide unravel the fine details of the mechanism of action of cytokines.

Keywords: IL-4; IL-10; receptor; interaction; regeneration; proximity ligation assay

1. Introduction

The understanding of the mechanisms of inflammation and tissue regeneration after wounding (irradiation, traumatic injury, and infection) is of great scientific and clinical interest. Immune cells form heterogeneous cell populations that acquire functional specialization in response to changes in the microenvironment [1–3]. Immune cells have long been known to induce inflammation and coordinate the efficient repair of damaged tissues [4–6]. However, the molecular and cellular mechanisms by which they exert their effects remain incompletely understood. If regeneration is not coordinated, fibrosis can occur [7,8]. Therefore, studying immune cell communication using different biological, molecular, and cellular approaches is important for the development of therapeutic strategies to repair tissues.

Cytokines secreted by immune cells have been shown to enhance tissue regeneration. Cytokines can be pro- or anti-inflammatory cytokines. Pro-inflammatory cytokines (IL-1β, TNF, and IFN-γ) promote the progression of inflammation in the early stages of inflammation. In contrast, anti-inflammatory cytokines (IL-4, IL-10, and IL-13) play a role in inhibiting inflammatory processes and promoting tissue regeneration.[9,10] IL-4, discovered in 1981, is a secreted cytokine [11,12]. CD4 T-cells, basophils, eosinophils, mast cells, NK T- and innate lymphoid cells 2 (ILC2) are the main IL-4 producers (Figure 1, Table 1) [13–19].

Preprints (www.preprints.org) | NOT PEER-REVIEWED | Posted: 23 April 2023 doi:10.20944/preprints202304.0741.v1

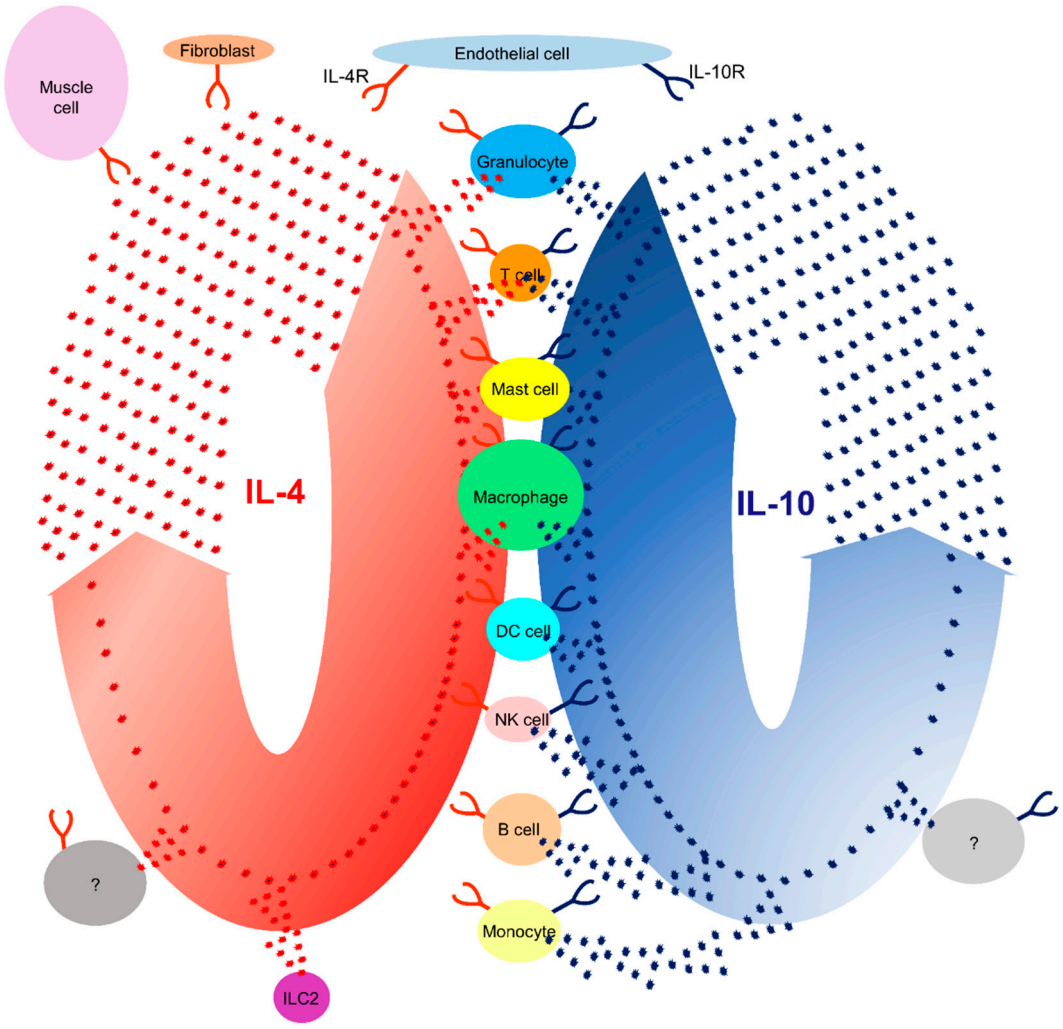

Figure 1. IL-4 and IL-10 cytokines are secreted by immune cells and their specific receptors. A schematic drawing of cells secreting IL-4 (red) or IL-10 (blue) and cells expressing the IL-4R and IL-10R.

Cytokine receptor-bearing cells respond to cytokines. The IL-4R is ubiquitously expressed and has been detected at the surface of B cells, T cells, mast cells, eosinophils, basophils, monocytes, macrophages, and non-lymphohematopoietic cells (fibroblasts, endothelial cells, airway epithelial cells, smooth muscle cells, and keratinocytes) (Figure 1, Table 1).[19–22] IL-13, also binds to the IL-4R and triggers a different signaling pathway [20].

Table 1. Expression of the IL-4 and IL-10 and their specific receptors. IL-4 in red, IL-10 in blue.

Expression	**IL-4**		**IL-10**	
	Cytokine	Receptor	Cytokine	Receptor
Granulocyte	+	+	+	+
T cell	+	+	+	+
Mast cell	+	+	+	+
Macrophage	+	+	+	+

Preprints (www.preprints.org) | NOT PEER-REVIEWED | Posted: 23 April 2023 doi:10.20944/preprints202304.0741.v1

Monocyte	-	+	+	+
B cell	-	+	+	+
DC cell	-	+	+	+
NK cell	-	+	+	+
ILC2	+	-	-	-
Endothelial cell	-	+	-	+
Fibroblast	-	+	-	-
Muscle cell	-	+	-	-

IL-10 was discovered 30 years ago by Fiorentino and colleagues (1989) [23]. They showed that IL-10 was secreted by T-helper Th2 cell clones and inhibited cytokine production by Th1 cells [23]. IL-10 was also found to be secreted by CD4 and CD8 T cells, B cells,[24] macrophages, monocytes, dendritic cells (DC), neutrophils, mast cells, eosinophils and natural killer cells (Figure 1, Table 1) [25–28]. In addition, some non-hematopoietic cells, epithelial cells, and tumor cells could also produce IL-10 [29]. IL-10 is a multifunctional cytokine; its main function is to suppress inflammatory responses. In addition, it regulates the function of monocytes, macrophages, B cells, NK cells, cytotoxic and helper T cells, mast cells, granulocytes, dendritic cells, keratinocyte,s and endothelial cells (Figure 1; Table 1) [25–28,30]. IL-10 is recognized by its cytokine-specific receptor [31].

Studies have also shown that cytokines act in coordination ensuring the effectiveness of tissue regeneration. Although the mechanism of action of cytokines is not fully unraveled, cytokines are known to act by binding to their cognate receptors (Figure 1). The activation of cells is regulated by the interaction of the receptors with cytokines [32]. Therefore, in animals and other organisms, the localization of cytokines *in situ* is not sufficient to understand the different steps of inflammation and tissue regeneration.

A special type of immune cell is the macrophage and more particularly tissue-resident macrophage, which, in addition to playing a role in homeostasis play an important role in the regeneration processes by continuously monitoring internal and external signals [33]. The other large group of macrophages that is located in the injured area is monocyte-derived macrophages [34]. Both tissue-resident and monocyte-derived macrophages can evolve into different phenotypes depending on their mode of activation [35]. This polarization is influenced *in vitro* by several cytokines (Figure 2A). In 1992, Gordon and coworkers demonstrated that IL-4 initiated M2 macrophage polarization of peritoneal macrophages, in contrast to IFN-γ which polarized them into M1 macrophages [36–38]. In 1995, IL-13 was identified as the cytokine that shares some functionality with IL-4 [39]. Over the years, other M2 macrophage activating factors were described (IL-4/IL-13 for M2a, IL-1R agonists/Toll-like receptor for M2b, IL-10 for M2c, and IL-6 for M2d) [9]. However, the mechanism of polarization *in vivo* is not well understood (Figure 2B) [40]. M1 macrophages and M2 macrophages have distinct roles in tissue regeneration [41]. M1 macrophages produce pro-inflammatory cytokines involved in tissue clearing to remove pathogens through phagocytosis, which would otherwise maintain inflammation [42]. The tissue regeneration phase is characterized by the change in phenotype of M1 macrophages into M2 macrophages that increase in number by producing anti-inflammatory cytokines, such as IL-10 and TGF-β [43]. M2 polarization of macrophages up-regulate the expression of the mannose receptor (CD206) [36,37]. *In situ*, the differentiation between tissue-resident and M2/M2-like macrophages is quite complicated because both express the CD206 marker [3,44].

Preprints (www.preprints.org) | NOT PEER-REVIEWED | Posted: 23 April 2023 doi:10.20944/preprints202304.0741.v1

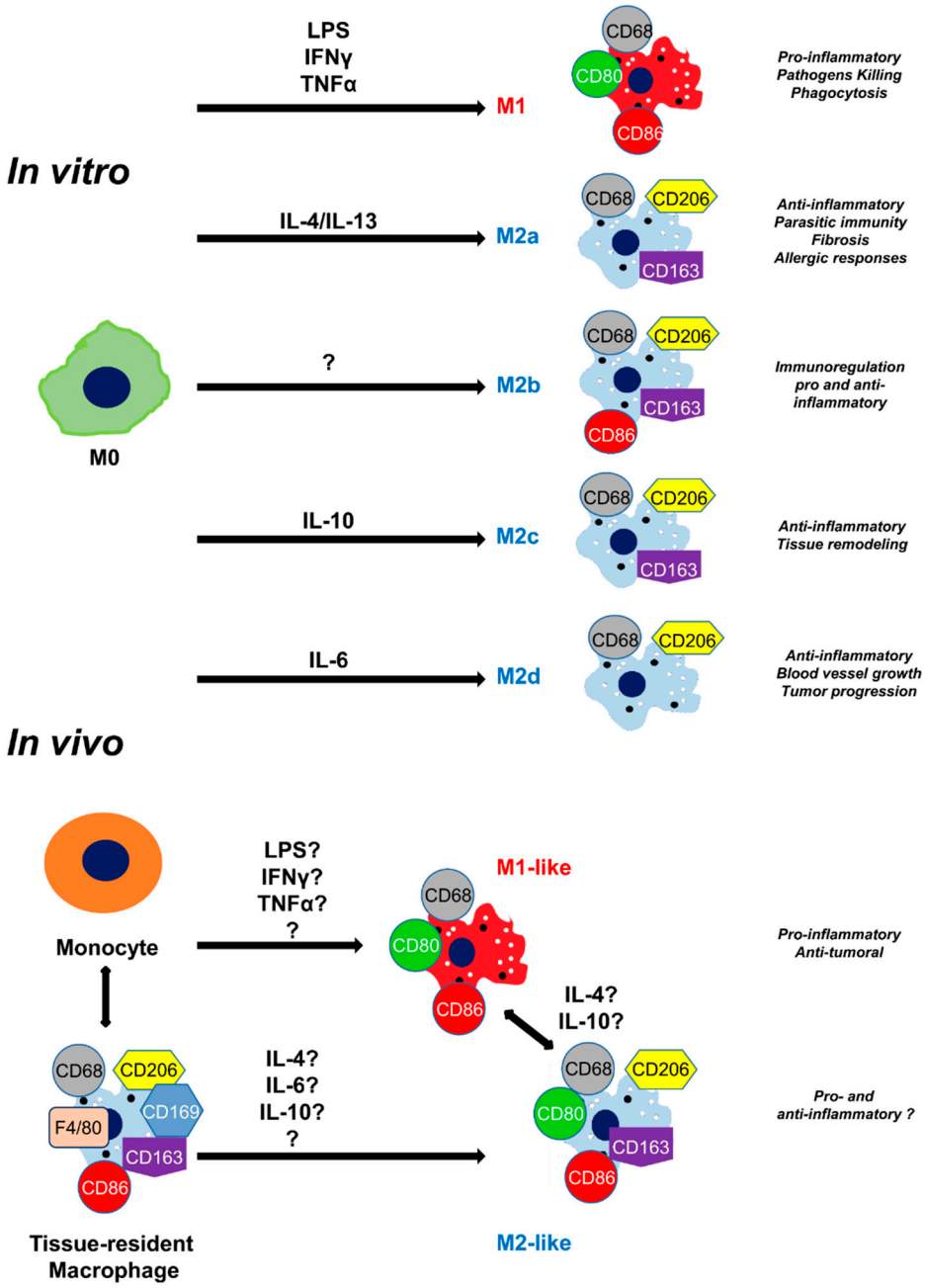

Figure 2. Macrophage activation and classification. *In vitro* and *in vivo* macrophage polarization depending on the activation pathway. M0: non-activated macrophage.

Several methods already exist to study protein-protein interactions *in vivo* with advantages and limitations: i) yeast two-hybrid systems are often used to identify protein-protein interactions *in vivo* [45]. However, the post-transcriptional modifications of some proteins may differ in yeast from those of animal cells, even if it is a eukaryote system. Moreover, it is not adapted to detect receptor-binding proteins. Therefore, protein-protein interactions observed by such methods may differ from the actual *in situ* interactions; ii) Forster resonance energy transfer (FRET) to study *in situ* analysis of protein-protein interactions [46]. However, this technique is somewhat cumbersome due to the autofluorescence in the cells; iii) Bimolecular fluorescence complementation (BiFC) is a very efficient technique but requires chimeric protein for analysis [47]; iv) Therefore, we were interested in a new

 doi:10.20944/preprints202304.0741.v1

innovative method, the proximity ligation assay (PLA) that allows the detection *in situ* of specific interaction events within protein complexes. In this technique, a couple of designed antibodies (each antibody is conjugated to oligonucleotides) bind *in situ* to two target proteins, suspected to interact with each other [48–52]. The oligonucleotides through a polymerase-mediated rolling circle reaction can be amplified and labeled with a fluorophore. The resulting fluorescence confirms the interaction between two proteins of interest. The advantage of the PLA method is the higher sensitivity and specificity compared with the FRET technic [32]. Although PLA has many advantages, one of its major disadvantages is its dependence on enzymes, which makes the method expensive and imposes requirements on enzyme storage and stability.

Our work aims to investigate the *in situ* interaction of two key anti-inflammatory cytokines (IL-4 and IL-10) and their receptors during tissue regeneration using a proximity ligation assay (PLA). Currently, little information is available on mammalian M2 macrophages, other than rodents and humans. The pig has proved to be an excellent model for understanding human macrophages, as tissue regeneration in the pig is very close to that in humans [53–55]. Therefore, three inflammatory pig models were studied to determine whether the observed interactions were general or wound-specific: skin tissue from an injured ear, infected lung, and irradiated skeletal muscle tissue, respectively. The challenging detection of the cytokine-receptor interaction *in situ* was a success that could provide new insights into cellular activation during tissue regeneration.

2. Materials and Methods

2.1. Tissue samples

This study was approved by the French Army Animal Ethics Committee (N°2011/22.1). All pigs were treated in compliance with the European legislation (dir 2010/63/EU) implemented into French law (decree 2013-118) regulating animal experimentation. Three kinds of tissues were selected: i) Skeletal muscle tissue from mini-pigs irradiated locally in the lumbar region with 60 cobalt sources at a dose rate of 0.6Gy/min up to 50Gy in the entry area. The irradiated muscles were harvested on day 76 after irradiation [56]; ii) lung tissue was collected from an animal with several signs of lower respiratory tract infection; iii) 2 days after the injury, skin tissue was collected from the ear that received a small voluntary cut.

2.2. Histological Staining

Histological staining was performed as described in [57]. Hematoxylin, phloxine, and saffron (HPS) staining were performed as follows: sections were embedded in 40 s hemalum (11,487, Merck, Darmstadt, Germany) buffer (0. 2 g hemalum, 5 g aluminum potassium sulfate in 100 ml distilled water), 3 min in water, 30 s in phloxine (15,926, Merck, Darmstadt, Germany) buffer (0.5 g phloxine in 100 ml distilled water), 1 min in water, 2 min in 70% ethanol, 30 s in 95% ethanol, 1 min in 100% ethanol and 1 min in 100% ethanol. The samples were put in saffron buffer for 10 minutes (6 g saffron (S8381, Sigma, Lezennes, France) in 200 ml absolute ethanol) and rinsed with absolute ethanol. Finally, the nuclei were dyed blue, the cytoplasm pink, and the tissue conjunctive orange.

2.3. Immunolabeling

Two types of immunolabeling were performed, one by enzymatic reaction (horseradish peroxidase) and the other by fluorescence detection. For both methods, muscle, skin, and lung tissues were harvested immediately after sacrifice and immersed in a fixative solution ANTIGENFIX (P0014, DiaPath, Martinengo, Italy) for 24 hours at 4 °C. After three washes with PBS (phosphate-buffered saline without Ca and Mg, GAUPBS0001, Eurobio, Les Ulis, France), samples were embedded in paraffin (39602004, Paraplast plus, Leica, Stuttgart, Germany). Sections of 5 µm were cut from the samples using a microtome (HistoCore, MulticutR, Leica, Stuttgart, Germany). The deparaffinization was carried out by successive 5 min washes (twice in 100% xylene, two times in 100% ethanol, two times in 95% ethanol, then in water). To restore the antigenicity of the proteins, sections were incubated with 10 mM citrate (pH:6.0) (AP0533-500, L-Recovery, Aptum, Boulogne-Billancourt,

France) in a steam oven for 15 min. After three washes in PBS, the sections were permeabilized for 15 min with 0.5% (v/v) Triton X100 (112298, Merck, Darmstadt, Germany) buffered with PBS. After three washes with PBS, non-specific binding was blocked with Emerald Antibody Diluent (936B-08, Sigma, Lezennes, France) for 1 hour. Then, sections were incubated overnight at 4°C with the primary antibody as follows: the primary goat anti-CD206 (C20) (sc-34577, Santa Cruz Bio. , Heidelberg, Germany) at 1:500 dilution; primary rabbit anti-IL-4R (ab203398, Abcam, Amsterdam, Netherlands) at 1:200 dilution; primary mouse anti-IL-4 (ab239508, Abcam, Amsterdam, Netherlands) at 1:500 dilution; primary rabbit anti-IL-10R (ab225530, Abcam, Amsterdam, Netherlands) at 1:500 dilution, and primary mouse anti-IL-10 (ab25075, Abcam, Amsterdam, Netherlands) at 1:200 dilution. The sections were washed three times in PBS for 10 minutes.

In one part, sections for enzymatic immunolabeling were treated with a 10-fold dilution of H2O2 (H1009, Sigma-Aldrich, Lezennes, France) for 20 min to inhibit endogenous hydrogen peroxidase. After three PBS washes, the slides were incubated with ready-to-use anti-Goat IgG horseradish peroxidase reagent (ImmPRESS MP-7405, Eurobio, Les Ulis, France) and counterstained with 3,3'-diaminobenzidine (DAB) (SK-4100, Eurobio, Les Ulis, France) and hematoxylin. Horseradish peroxidase oxidizes DAB, turning it brown and detectable, thus allowing the detection of macrophages. Labeling was detected with a DM6000 epifluorescence microscope (Leica, Stuttgart, Germany) equipped with a monochrome and color digital camera.

In a second part, sections for fluorescent immunolabeling were incubated with a 1:1000 dilution of Alexa Fluor 488 (A-21206, Thermo Scientific, Villebon sur Yvette, France) anti-rabbit secondary antibody and a 1:1000 dilution of Alexa Fluor 568 (ab175704, Abcam, Amsterdam, Netherlands) anti-goat secondary antibody for 2 hours at room temperature. Finally, tissue sections were washed three times in PBS for 10 min and subsequently mounted with Fluoroshield mounting medium supplemented with DAPI (ab104139, Abcam, Amsterdam, Netherlands). Fluorescence was detected with a confocal microscope (LSM700, Zeiss, Dresden, Germany).

2.4. Proximity ligation assay (PLA)

The sections were fixed, antigen retrieved and permeabilized as described in the immunolabeling section. To detect protein-protein interactions, the Duolink® *in situ* red starter kit Mouse/Rabbit (DUO92101-1KT, Sigma-Aldrich, Lezennes, France) was used according to the company's recommendations. Briefly, the samples were blocked with Duolink® blocking solution for 60 min at 37 °C. Then, sections were incubated overnight at 4°C with the primary antibody as follows: primary rabbit anti-IL-4R (ab203398, Abcam, Amsterdam, Netherlands) at 1:200 dilution; primary mouse anti-IL-4 (ab239508, Abcam, Amsterdam, Netherlands) at 1:500 dilution; primary rabbit anti-IL-10R (ab225530, Abcam, Amsterdam, Netherlands) at 1:500 dilution, and primary mouse anti-IL-10 (ab25075, Abcam, Amsterdam, Netherlands) at 1:200 dilution. Primary antibodies were diluted with Duolink® antibody diluent. The sections were washed three times in wash buffer A for 10 minutes. The secondary antibodies used are bound to DNA oligonucleotides. These antibodies are called PLA probes. One of the two probes is PLUS (+) and the other is MINUS (-). The sections were then incubated with Duolink® plus and minus PLA probes for 60 min at 37°C. DNA oligonucleotides linked to the secondary antibody were ligated for 30 min at 37°C (Duolink® ligase) into circular DNA using hybridizing connector oligonucleotides. The sections were washed three times for 5 minutes in wash buffer A at room temperature. The circular DNA was amplified by Duolink® polymerase at 37 °C for 100 min. Finally, tissue sections were washed two times in wash buffer B for 10 min and subsequently mounted with Duolink® mounting medium supplemented with DAPI.

2.4. Quantification and statistical analysis

Quantitative studies were based on random immunofluorescence assays, analyzing 3 times 1000 cells in different tissues.

All statistical calculations were performed with a one-way analysis of variances (ANOVA) using GraphPad PrismVersion 4.0 [58]. Post-test comparisons, performed only if $p<0.05$, were made using Bonferroni's Multiple Comparison Test. Chi 2.

Preprints (www.preprints.org) | NOT PEER-REVIEWED | Posted: 23 April 2023 doi:10.20944/preprints202304.0741.v1

3. Results

3.1. Tissue wounds induce endothelial cell activation and immune cell infiltration

Rodents are commonly used as animal models to study tissue regeneration, but little information is available for other animal models. Interestingly, tissue regeneration in humans is more similar to that in pigs than it is to that in rodents [53–55,59]. Therefore three tissues from a pig animal model were selected to perform this study (skin, lung, and muscle) and histological staining was used to characterize the morphology (Figure 3).

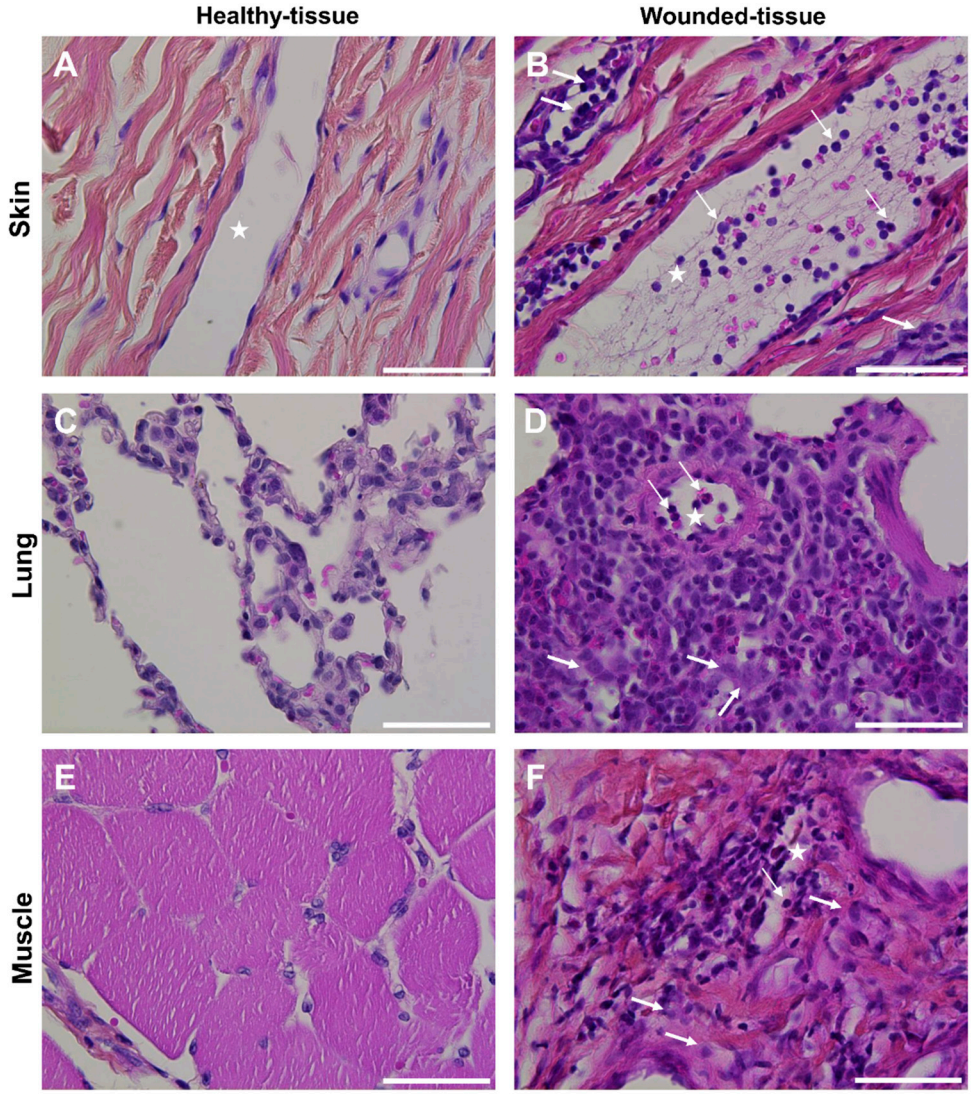

Figure 3. Macroscopic morphology of tissues. Histologic HPS staining was performed on (**A,B**) skin (**C,D**) lung and (**E,F**) muscle sections in (**A,C,E**) healthy-tissue and (**B,D,F**) wounded-tissue. Scale bar = 50 μm. Thin arrow: granulocyte; thick arrow: macrophage; star: lumen of the blood vessel.

Strong endothelial cell activation and intense immune cell infiltration were observed in the wounded tissues (Figure 3B,D,F) compared to healthy tissues (Figure 3A,C,E). The infiltration was mainly localized around blood vessels (Figure 3B,D,F). In the skin and lungs, many granulocytes were observed in the lumen of the vessels (Figure 3B,D). In contrast, no granulocytes were observed in the lumen of the vessels or other parts of the wounded-muscle tissue (Figure 3).

Preprints (www.preprints.org) | NOT PEER-REVIEWED | Posted: 23 April 2023 doi:10.20944/preprints202304.0741.v1

3.2. Tissue damage results in the accumulation of M2 macrophages around the blood vessel

As histological staining only assumes the presence of macrophages based on cell morphology, immunolabeling with macrophage-specific antibodies is required for their identification.

First, the CD206 marker, highly expressed by the M2 phenotype of macrophages in injured tissues, was used to check the activation of M2 macrophages (Figure 4). The specificity of the anti-CD206 antibody was validated by the lack of signal obtained in the negative control (Figure 4A,C,E,G,I,K).

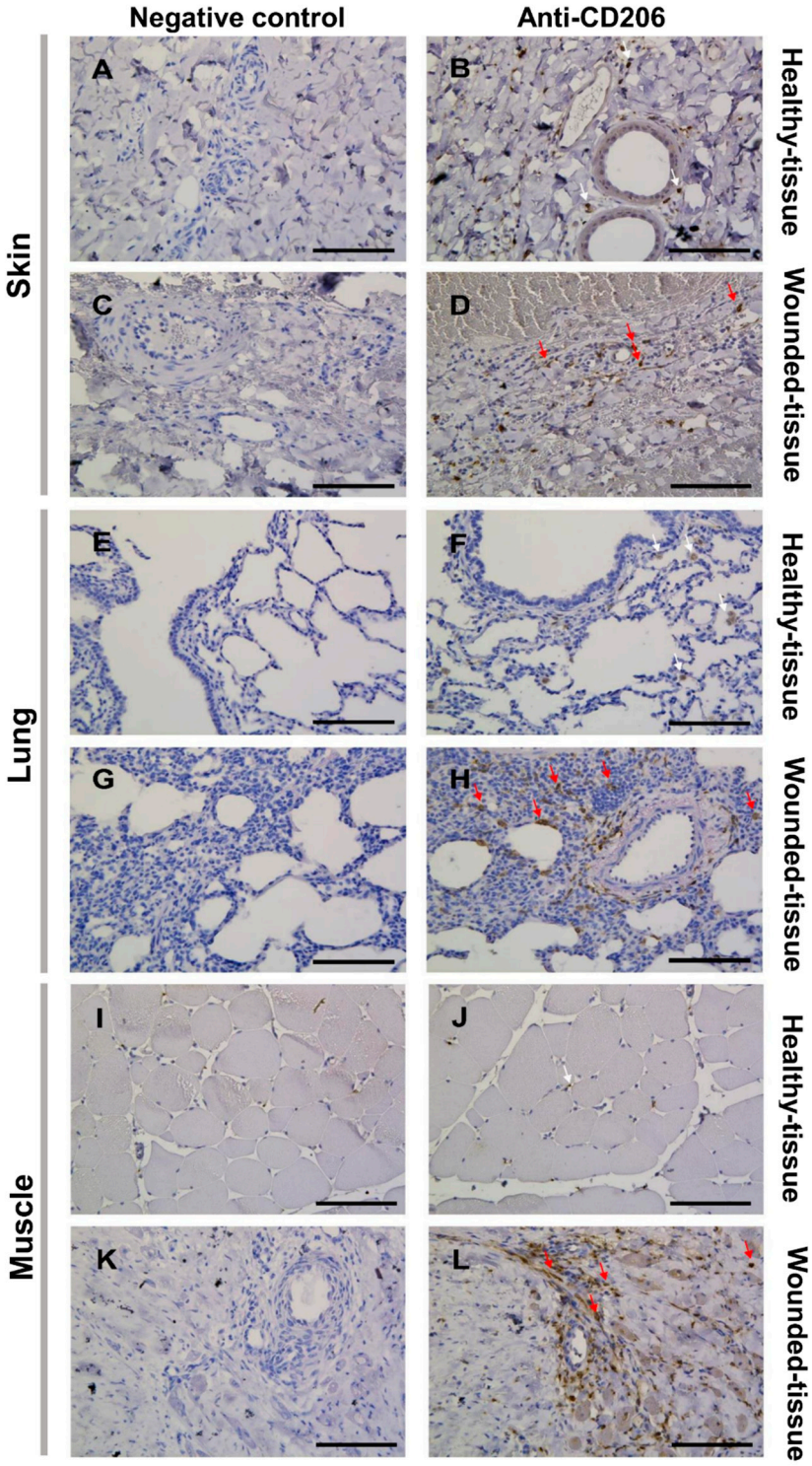

Figure 4. Identification of tissue-resident and M2-like macrophages *in situ*. (**B, D, F, H, J, L**) Immunolabeling with CD206 of the (**A-D**) skin of the (**E-H**) lung and the (**I-L**) muscle sections.

 doi:10.20944/preprints202304.0741.v1

(**A,B,E,F,I,J**) Healthy-tissue. (**C,D,G,H,K,L**) Wounded-tissue. (**A,C,E,G,I,K**) Negative controls of the immunolabeling. (**B,D,F,H,J,L**) Anti-CD206 (brown color) labeling the tissue-resident and M2-like macrophages. Nuclear staining with hematoxylin (blue color). Scale bar = 100 μm. White arrow: Tissue-resident macrophage; red arrow: M2-like macrophage.

Since immunolabeling does not allow distinction of macrophage types, cells expressing the CD206 marker in healthy tissues were assumed as tissue-specific or tissue-resident macrophages, which are always present but not activated (Figure 4B,F,J) [33,34,60]. Indeed, in healthy tissue, macrophage polarization does not occur (Figure 4B,F,J). However, the expression of CD206 in treated tissue may label M2-like macrophages which are highly activated during regeneration (Figure 4D,H,L).

Overall, damaged tissue generates a higher activation of macrophages compared to healthy tissue, as there are more CD206-positive (CD206+) cells in damaged tissue than in healthy tissue. This is particularly evident around blood vessels. In addition, the sphericity of the endothelial cell nuclei showed that the tissues have been exposed to inflammation and the endothelial cells have been activated (Figure 4D,H,L).

3.3. Tissue injury activates IL-4R expression on the surface of macrophages

Recently, the IL-4 cytokine has been the focus of attention because of its key role in tissue regeneration [61]. Under *in vitro* conditions, IL-4 cytokine can be used to polarize M2a macrophages from monocytes [62]. In a second step, we examined whether tissue injury activates IL-4R expression on the surface of macrophages under *in vivo* conditions. For this experiment, the CD206/IL-4R co-localization was investigated in the skin, muscle, and lung wounded tissues, with the CD206 marker labeled in red, the IL-4R labeled in green, and the nuclei labeled in blue. The co-localization of both IL-4R and CD206 proteins was studied by immunofluorescence to obtain double labeling on the same tissue sample. In the absence of a primary antibody (negative control), no expression of these markers was observed (Figure S1).

In the skin sample, (Figure 5A,B), mainly two types of cells were observed, macrophages (CD206+/IL-4R+ cells) (thin arrow) and endothelial cells (CD206-/IL-4R+ cells) (arrowhead) expressing the IL-4R in the internal surface of the blood vessel.

For the muscle sections, similar observations could be made (Figure 5E,F), with slightly higher levels of M2-like macrophages than in the skin sample.

Similarly, significant levels of macrophages expressing IL-4R protein (Figure 5I,J) were identified in the wounded lung. In the lumen of the blood vessels, immune cells showed strong IL-4R expression but were CD206 negative (Figure 5K). No granulocytes were observed since the latter does not express the IL-4R.

In summary, the three different injured tissues showed a very similar pattern. Indeed, there were significantly more M2-like macrophages expressing the IL-4R (CD206+/IL-4R+) in wounded-tissue (6.3% (skin); 11.4% (muscle); 9.1% (lung)) than in healthy tissues (1.6% (skin); 0.5% (muscle); 1.8% (lung) (Figure 5C,D,G,H,L,M)). Concomitantly, the number of M2-like macrophages without IL-4R (CD206+/IL-4R-) was significantly reduced (2.6% (skin); 7% (muscle); 2.5% (lung)) in wounded tissues compared to healthy tissues (8.5% (skin); 8.5% (muscle); 6% (lung)) (Figure 5C,D,G,H,L,M). Since M2-like macrophages express the IL-4R upon injury, it can be assumed that they are the main targets of the IL-4 cytokine. Moreover, other target cells were also identified during regeneration since an increase in CD206-/IL-4R+ cells was detected in wounded tissues (10.5% (skin); 5% (muscle); 5.8% (lung)) compared to the healthy tissue (7.7% (skin); 1.4% (muscle); 3.4% (lung) (Figure 5A,E,I).

Preprints (www.preprints.org) | NOT PEER-REVIEWED | Posted: 23 April 2023 doi:10.20944/preprints202304.0741.v1

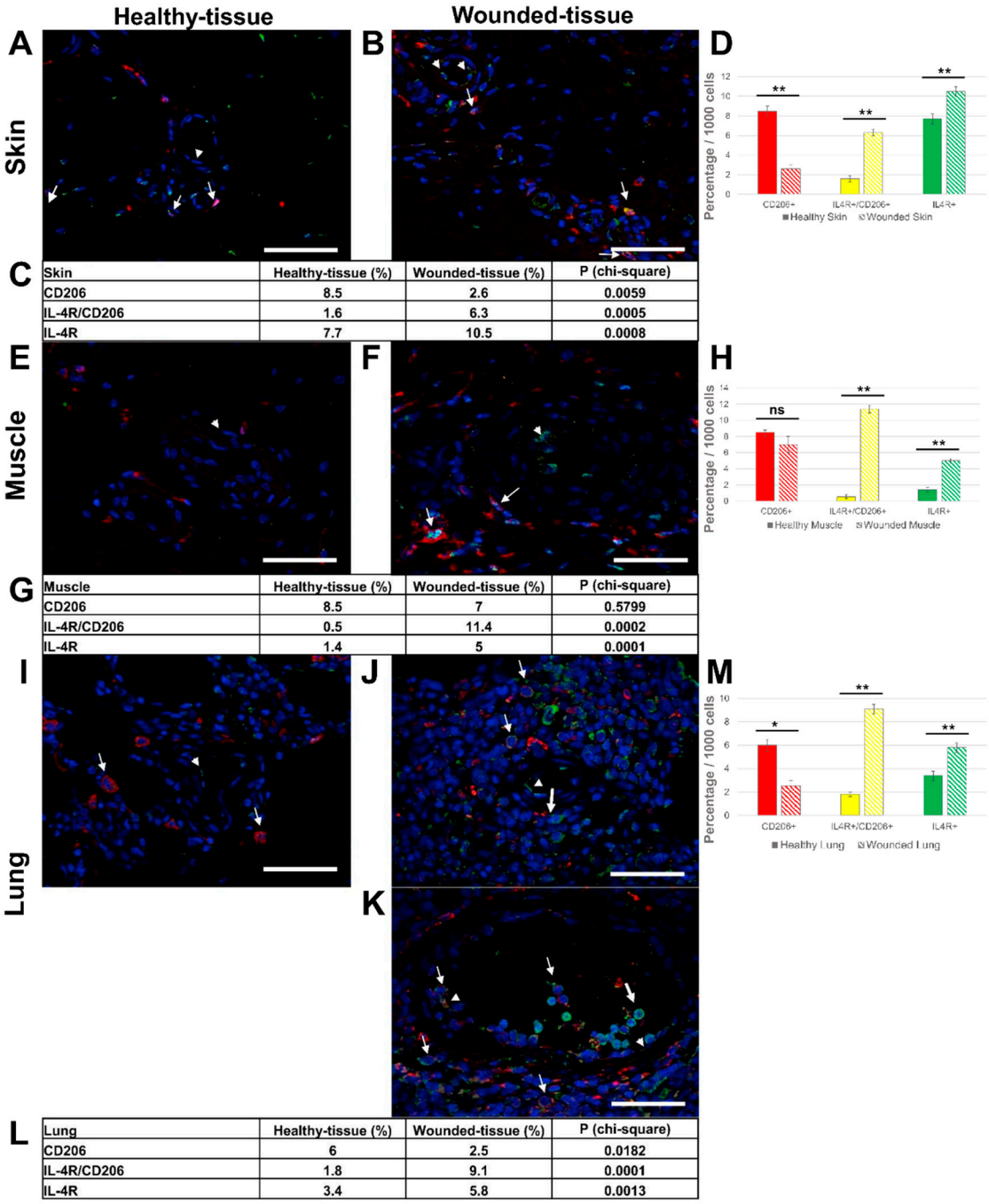

Skin	Healthy-tissue (%)	Wounded-tissue (%)	P (chi-square)
CD206	8.5	2.6	0.0059
IL-4R/CD206	1.6	6.3	0.0005
IL-4R	7.7	10.5	0.0008

Muscle	Healthy-tissue (%)	Wounded-tissue (%)	P (chi-square)
CD206	8.5	7	0.5799
IL-4R/CD206	0.5	11.4	0.0002
IL-4R	1.4	5	0.0001

Lung	Healthy-tissue (%)	Wounded-tissue (%)	P (chi-square)
CD206	6	2.5	0.0182
IL-4R/CD206	1.8	9.1	0.0001
IL-4R	3.4	5.8	0.0013

Figure 5. Identification of IL-4R+ and CD206+ cells *in situ*. (**A,B**) Immunolabeling of both IL-4R and CD206 in the skin, (**E,F**) the muscle, and (**I-K**) the lung sections. (**A,E,I**) Healthy-tissue. (**B,F,J,K**) Wounded-tissue. (**C,D**) Quantitative analysis of both IL-4R+ and CD206+ cells in the skin; (**G,H**) the muscle and (**L,M**) the lung. Quantitative analysis based on random examination of 3 sets of 1,000 cells per condition. Anti-IL-4R (Alexa488, green fluorescence) and Anti-CD206 (Alexa568, red fluorescence) labeling the tissue-resident and M2-like macrophages. Nuclear staining with DAPI (blue fluorescence). Scale bar = 50 µm. Arrowhead: endothelial cell; thin arrow: macrophage and thick arrow: IL-4R+ cell. ** $p < 0.01$, * $p < 0.5$, ns = not significant, compared to healthy-tissue.

Preprints (www.preprints.org) | NOT PEER-REVIEWED | Posted: 23 April 2023 doi:10.20944/preprints202304.0741.v1

3.4. Injury in muscle tissue displayed high IL-10R expression

IL-10 has been shown to play a key role in tissue regeneration by activating M2 macrophages and downregulating the production of pro-inflammatory cytokines. In the next experiment, we investigated the IL-10R expression on the surface of macrophages *in vivo*. The co-localization of IL-10R and CD206 proteins was studied by immunofluorescence (Figure 6), CD206/IL-10R co-localization, labeling the CD206 marker in red, the IL-10R in green and the nuclei in blue. In the absence of a primary antibody (negative control), no expression of these markers was observed (Figure S2). The number of IL-10R-expressing M2-like macrophages (CD206+/IL-10R+) was increased in wounded tissues (1.4% (skin); 11.3% (muscle)) compared to healthy tissues (0.2% (skin); 0.2% (muscle)) (Figure 6 C,D,G,H,M,N).

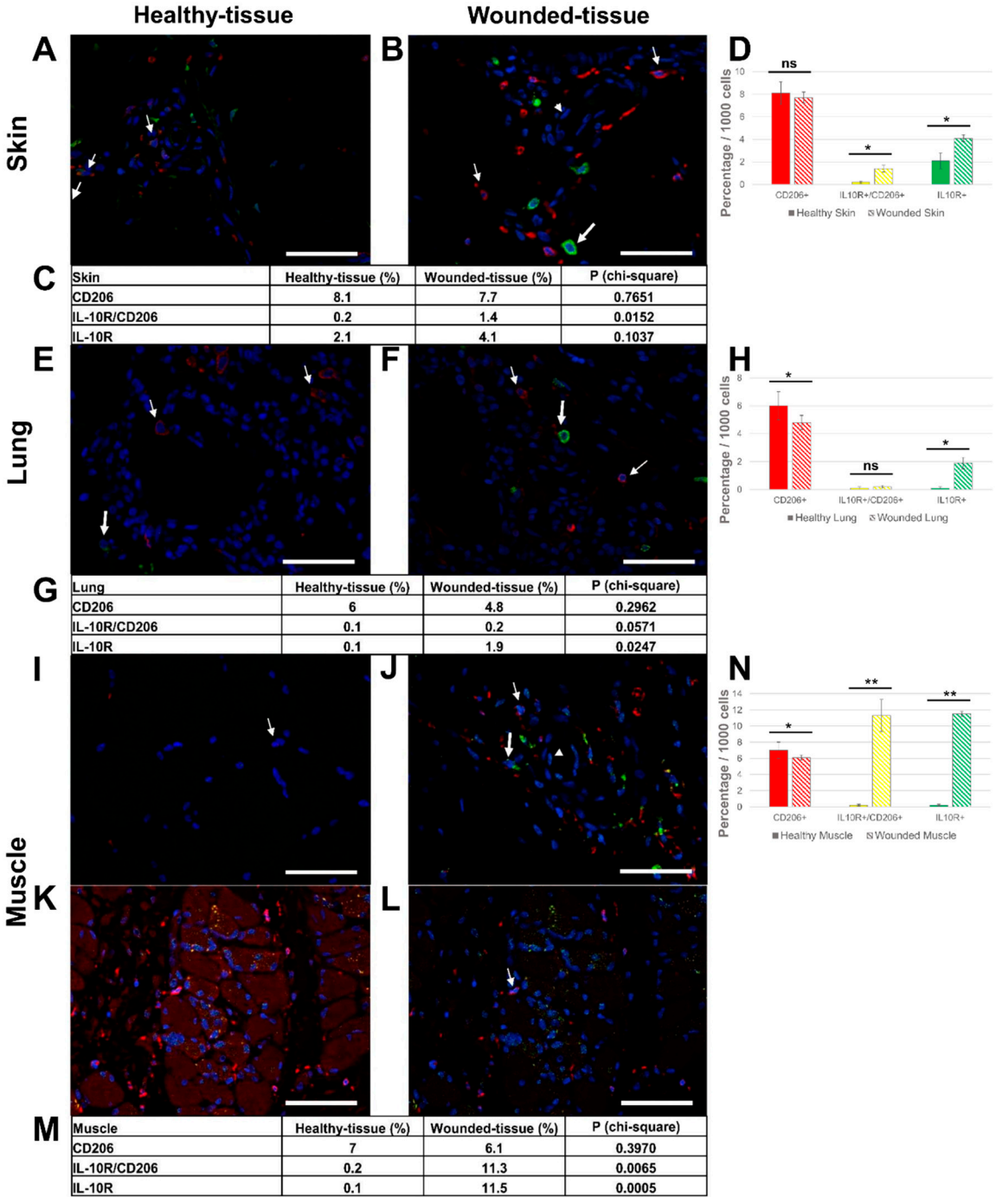

Skin	Healthy-tissue (%)	Wounded-tissue (%)	P (chi-square)
CD206	8.1	7.7	0.7651
IL-10R/CD206	0.2	1.4	0.0152
IL-10R	2.1	4.1	0.1037

Lung	Healthy-tissue (%)	Wounded-tissue (%)	P (chi-square)
CD206	6	4.8	0.2962
IL-10R/CD206	0.1	0.2	0.0571
IL-10R	0.1	1.9	0.0247

Muscle	Healthy-tissue (%)	Wounded-tissue (%)	P (chi-square)
CD206	7	6.1	0.3970
IL-10R/CD206	0.2	11.3	0.0065
IL-10R	0.1	11.5	0.0005

Figure 6. Identification of IL-10R+ and CD206+ cells *in situ*. (**A,B**) Immunolabeling of both IL-10R and CD206 in the skin, (**E,F**) the lung, and (**I-L**) the muscle sections. (**L**) identical to the K image, including

 doi:10.20944/preprints202304.0741.v1

the autofluorescence of muscle cells. (**A,E,I**) Healthy-tissue. (**B,F,J,K,L**) Wounded-tissue. (**C,D**) Quantitative analysis of the IL-10R+ and CD206+ cells in the skin; (**G,H**) the lung and (**M,N**) the muscle. Quantitative analysis based on random examination of 3 sets of 1000 cells per condition. Anti-IL-10R (Alexa488, green fluorescence) and Anti-CD206 (Alexa568, red fluorescence) labeling the tissue-resident and M2-like macrophages. Nuclear staining with DAPI (blue fluorescence). Scale bar = 50 μm. Arrowhead: endothelial cell; thin arrow: macrophage and thick arrow: IL-10R+ cell. ** $p < 0.01$, * $p < 0.5$, ns = not significant, compared to healthy-tissue.

The number of M2-like macrophages without IL-10R (CD206+/IL-4R-) was reduced (7.7% (skin); 6.1% (muscle); 4.8% (lung)) in wounded tissues compared to healthy tissues (8.1% (skin); 7% (muscle); 6% (lung) (Figure 6C,D,G,H,M,N)). Moreover, other target cells were also present during regeneration as an increase in the number of CD206-/IL-10R+ cells was observed in damaged tissue (4.1% (skin); 11.5% (muscle); 1.9% (lung)) compared to healthy tissues, respectively (2.1% (skin); 0.1% (muscle); 0.1% (lung) (Figure 6C,D,G,H,M,N)).In addition, regenerating muscle cells showed intense IL-10R expression (Figure 6K,L).

3.5. Granulocytes show high IL-4 expression

The co-localization between IL-4 and IL-4R was studied in skin, lung, and muscle tissues (Figure 7 and Figure S3). IL-4 is labeled in red, its receptor in green and the nuclei are labeled in blue (Figure 7 and Figure S3). In the absence of a primary antibody (negative control), no expression of these markers was observed (Figure S4).

For the skin tissue, (Figures 7A,B), two types of IL-4+ cells were identified (IL-4+ cells): i) granulocytes (thin arrow), expressing a high level of IL-4 in the cytoplasm; ii) cells detected around the vessel, expressing both IL-4 and IL-4R. Because cytokines can simultaneously be secreted and activate the same cell, it was more difficult to recognize IL-4-secreting cells than IL-4-targeted cells (Figure 7A,B).

Regarding the lung (Figures 7C,D), granulocytes and IL-4+/IL-4R+ cells were detected, but in lower levels compared to the skin. All around the lumen of the blood vessels (labeled with a star) were cells expressing IL-4. For the muscle section (Figures 7E,F), the co-localization of IL-4 and IL-4R was very intense only around the vessel.

Preprints (www.preprints.org) | NOT PEER-REVIEWED | Posted: 23 April 2023 doi:10.20944/preprints202304.0741.v1

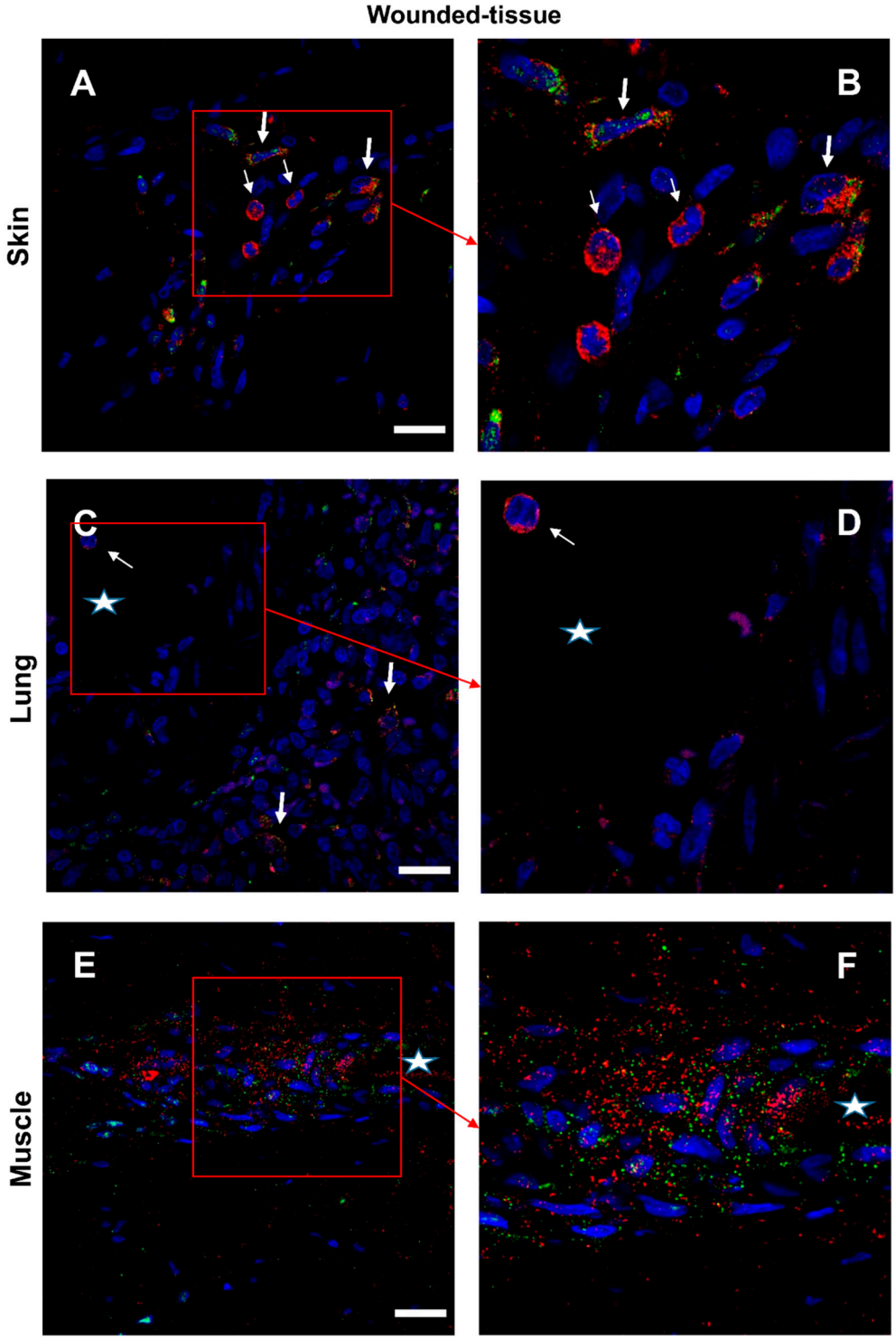

Figure 7. Identification of IL-4R+ and IL-4+cells *in situ*. (**A,B**) Immunolabeling of both IL-4R and IL-4 in the wounded skin, (**C,D**) the lung, and (**E,F**) the muscle sections. (**B,D,F**) Expanded view: high magnification image of the area within the red rectangle in A,C, and E respectively. Anti-IL-4R (Alexa488, green fluorescence) and Anti-IL-4 (Alexa568, red fluorescence). Nuclear staining with DAPI (blue fluorescence). Scale bar = 20 μm. Star: lumen of the blood vessel, thin arrow: IL-4+ granulocyte, and thick arrow: IL-4R+/ IL-4+ cell.

3.6. Expression of IL-10 cytokine in different tissues

The co-localization between the IL-10 cytokine and the IL-10R was confirmed (Figure 8 and Figure S5). In the absence of a primary antibody (negative control), no expression of these markers

Preprints (www.preprints.org) | NOT PEER-REVIEWED | Posted: 23 April 2023 doi:10.20944/preprints202304.0741.v1

was observed (Figure S6). In skin and lung tissues (Figures 8A-D), two types of cells were observed: IL-10R+ cells (thin arrow) and some IL-10+ cells (thick arrow)
Nevertheless, no co-localization of the two labels was observed. Granulocytes (arrowhead) in the lumen of the vessel did not express either IL-10 cytokine or IL-10R (Figure 8C).

In the muscle sample, several cells around the regenerating muscle were found to be IL-10R+ and IL-10+ positive (Figures 8E,F). However, since cytokines are secreted it is difficult to determine which cells are sources and which are targets of cytokines. Only protein-protein (cytokine-cytokine receptor) interactions can answer this question.

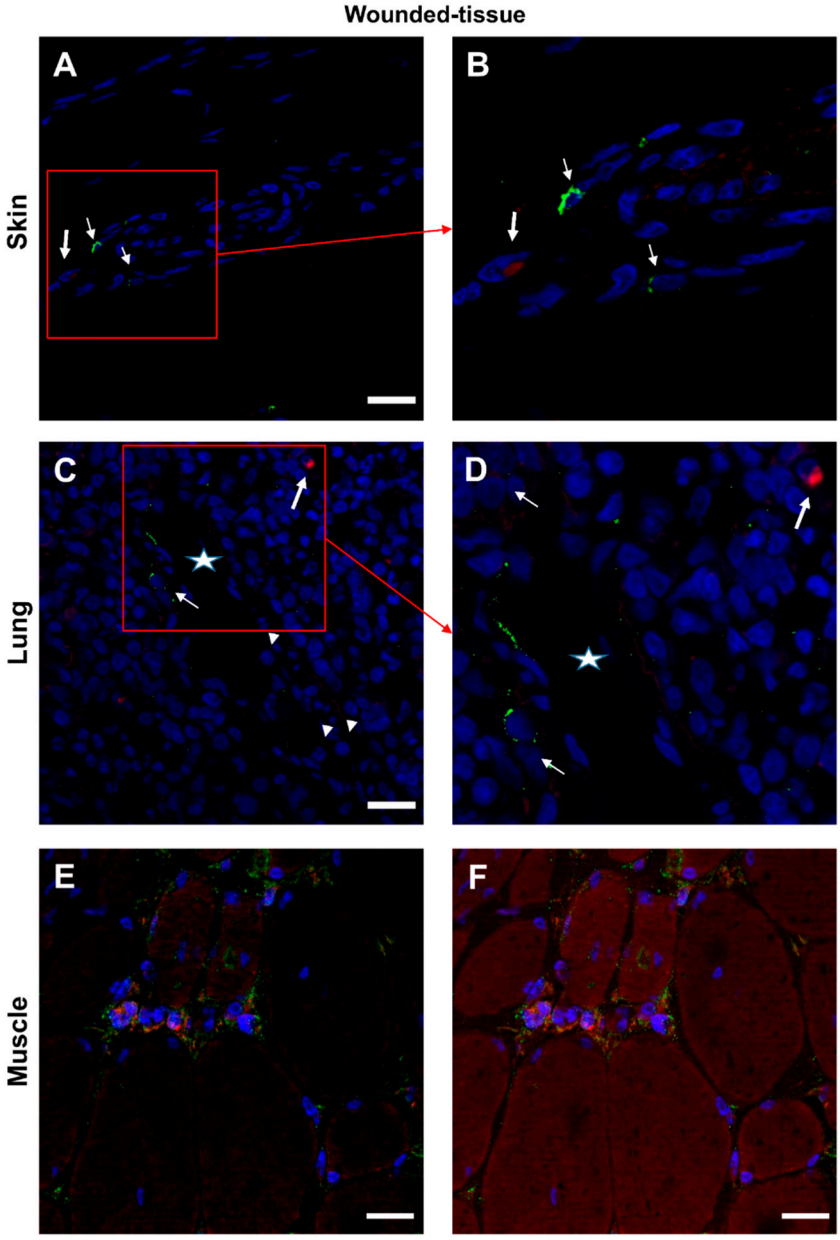

Figure 8. Identification of IL-10R+ and IL-10+ cells *in situ*. (**A,B**) Immunolabeling of both anti-IL-10R and IL-10 antibodies in the wounded skin, (**C,D**) the lung, and (**E,F**) the muscle sections. (**B,D**) Expanded view: high magnification image of the area within the red rectangle in A,C respectively. (**F**) identical to the E image, including the autofluorescence of muscle cells. Anti-IL-10R (Alexa488, green fluorescence) and Anti-IL-10 (Alexa568, red fluorescence). Nuclear staining with DAPI (blue fluorescence). Scale bar = 20 μm. Star: lumen of the blood vessel, arrowhead: granulocyte in the blood vessel, thin arrow: IL-10R+ cell, and thick arrow: IL-10+ cell.

Preprints (www.preprints.org) | NOT PEER-REVIEWED | Posted: 23 April 2023 doi:10.20944/preprints202304.0741.v1

3.7. IL-4/IL-4R and IL-10/IL-10R interaction in situ

Immunostaining is useful to specifically detect proteins while reliable indications regarding protein-protein interactions could be effectively studied by proximity ligation assays in order to identify, via the identified interaction, the target cells involved.

Interactions between the IL-4 cytokine and its respective receptor IL-4R (Figure 9 and Figure S7) and similar IL-10/IL-10R interactions (Figure 10 and Figure S8) were studied in the different sections. In the absence of a primary antibody (negative control), no protein-protein interaction was observed (Figure S9). In samples from healthy animals, cytokine-receptor interactions were detected in a few cells (Figure S7,8). In contrast, in wounded tissues, cytokine-receptor interactions were enhanced with very distinct patterns for the two cytokines (Figure 9,10). The interaction of IL-4/IL-4R was mainly activated around the vasculature (Figure 9) whereas the activation of IL-10/IL-10R was more localized to muscle cells (Figure 10E,F). Few granulocytes were observed in the vessel lumen without signs of interactions between the two proteins (Figure 9D). Some other immune cells showing a positive IL-4/IL-4R interaction were also observed in the lumen (Figure 9D). Similar results were also observed in the skin (data not shown).

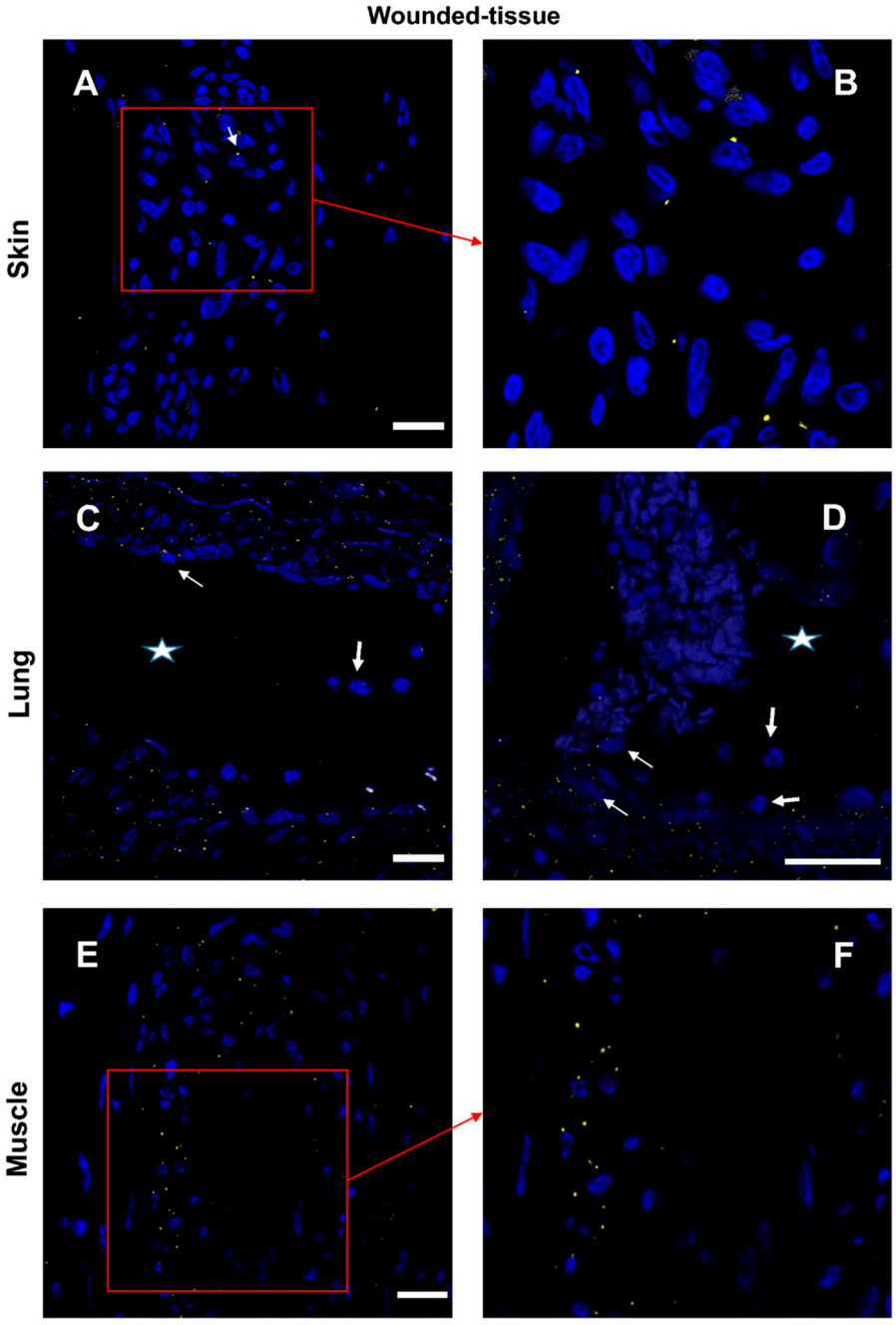

Preprints (www.preprints.org) | NOT PEER-REVIEWED | Posted: 23 April 2023 doi:10.20944/preprints202304.0741.v1

Figure 9. Interaction between IL-4 and IL-4R *in situ*. (**A,B**) Proximity Ligation Assay with anti-IL-4 and anti-IL-4R antibodies in the wounded skin, (**C,D**) the wounded lung, and (**E,F**) the wounded muscle. (**B,F**) Expanded view: high magnification image of the area within the red rectangle in A,E. Alexa568, yellow fluorescence, labeling the interaction between IL-4 and IL-4R. Nuclear staining with DAPI (blue fluorescence). Scale bar = 20 μm. Star: lumen of the blood vessel, thin arrow: Proximity Ligation Assay IL-4R+/IL-4+ cells, thick arrow: granulocyte.

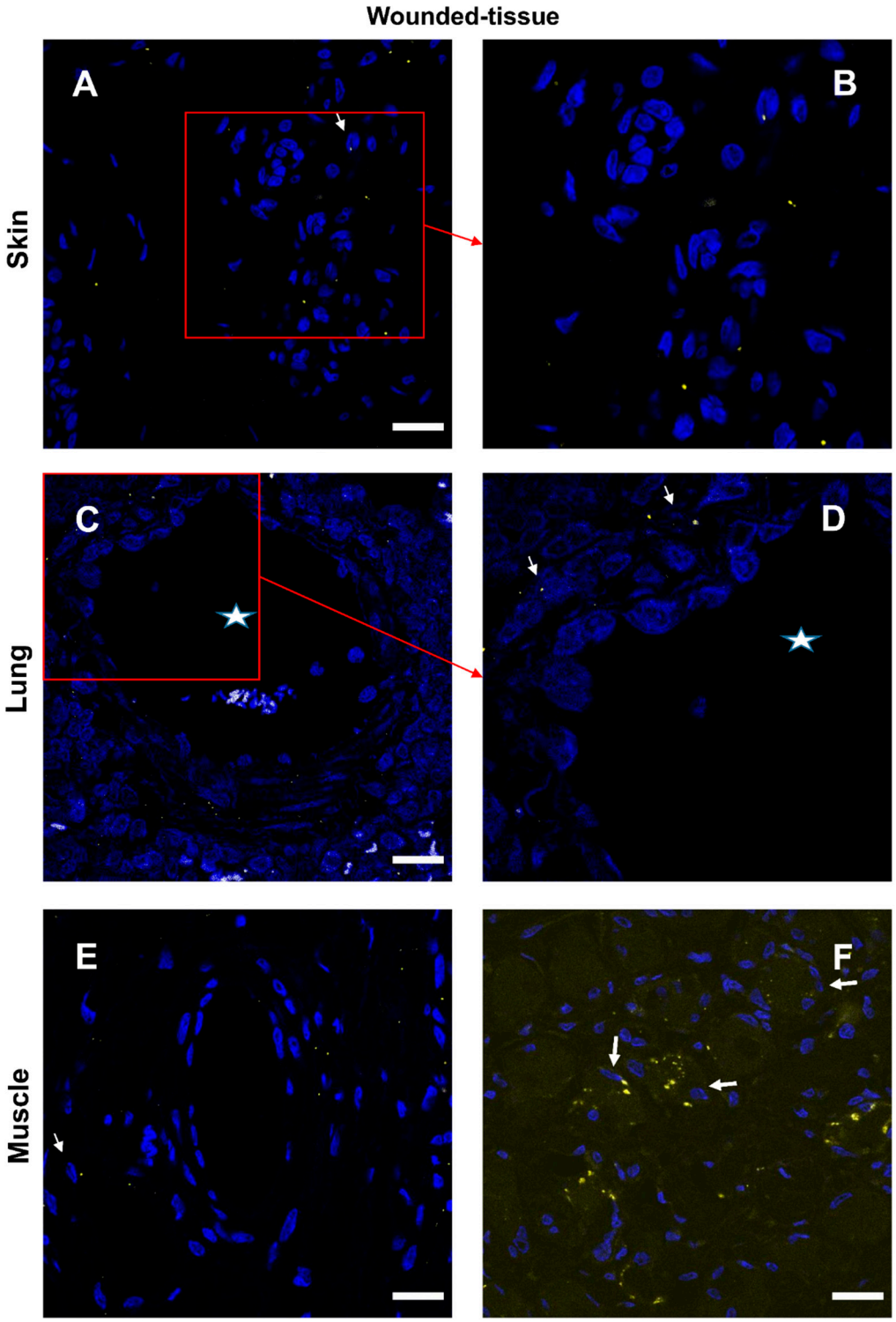

Figure 10. Interaction between IL-10 and IL-10R *in situ*. (**A,B**) Proximity Ligation Assay with anti-IL-10R and anti-IL-10 in the wounded skin (**C,D**) the wounded lung and (**E,F**) the wounded muscle. (**B,D**) Expanded view: high magnification image of the area within the red rectangle in A,C. Alexa568,

 doi:10.20944/preprints202304.0741.v1

yellow fluorescence, labeling the interaction between IL-10 and IL-10R. Nuclear staining with DAPI (blue fluorescence). Scale bar = 20 µm. Star: lumen of the blood vessel, thin arrow: Proximity Ligation Assay IL-10R/IL-10+ cells, thick arrow: muscle fiber.

4. Discussion

Macrophages play an important role in tissue development, homeostasis, and wound healing. Several phenotypes of macrophages were identified and each of them plays a distinct role during the tissue regeneration process through the expression of a panel of cytokines, [44,59,63,64] which have diverse roles in each process [43,59,62]. However, the mechanisms of communication between the immune effectors and the macrophages during tissue regeneration are still poorly understood *in vivo*. Indeed, *in vitro* observations could not be readily transposed to *in vivo* conditions because *in vivo* mechanisms are more complex [42].

In vitro, the addition of IL-10 to muscle cell cultures can enhance the percentage of myogenin-expressing cells and improve cell fusion [65]. Injection of both anti-inflammatory cytokines (IL-4 and IL-10) into injured tissue can significantly enhance wound healing in different tissues [26,66–68]. In addition, M2c macrophages express a high level of both IL-4 and IL-10, suggesting they play a significant role in promoting muscle regeneration.[8,37] *In vivo*, intramuscular injection of IL-10 DNA is effective in suppressing inflammation by inhibiting the production of proinflammatory cytokines [69–71]. In addition, IL-10 can promote myocardial cell regeneration [72] and skeletal muscle cell healing.[73] Myocytes are capable of co-expressing IL-10 and IL-10R, but this interaction has not yet been experimentally demonstrated under *in situ* conditions [74]. However, it should also be mentioned that these two cytokines can have a negative effect on tissue regeneration, depending on where, when, and in which animal model they were injected, making their use in therapeutic treatment difficult [21,75]. To make progress in this area, of a deeper understanding of the IL-4 and IL-10 cytokine-receptor interaction is needed. Cytokine therapy is an intensively developing field and exciting new advances in understanding the mechanism of action of these cytokines are expected in the future [76].

In our work, we aimed to address this question. Granulocytes are known to be a source of IL-4 [77]. We show that granulocytes in the skin and lungs are the primary IL-4 producers. Rare granulocytes were identified in muscle tissue, as this tissue was collected 76 days after irradiation. In these tissues, IL-4 production was mainly localized around the vasculature. For IL-10, many IL-10+ cells were identified in skin, lung, and muscle sections. No IL-10 expression was detected in granulocytes. Identifying cells expressing both IL-4 and IL-10 will be a task in the future.

The expression of cytokine receptors was also analyzed in healthy tissues (skin, lung, and muscle), IL-4R and IL-10R were weakly but ubiquitously present in different cell types, similar to the findings reported in the literature [78,79]. However, in the different regenerating tissues (regardless of the source of injury), the expression of both receptors
was intensely increased at the surface of macrophages. These results suggest that similarly to the *in vitro* results, the activity of these two cytokines is essential for the polarization of macrophages *in vivo* (Figure 2). In the future, to verify whether the cytokine-receptor interactions also occur in macrophage cells, combined protein-protein interaction with the CD206 immunolabeling of macrophages could be performed. It would also be interesting to detect which subtypes of macrophages are most involved in polarization. As classical
immunolabelling is not able to distinguish M2 macrophage subtypes *in situ*, future work will focus on the identification of macrophage subtypes by *in situ* hybridization [42].

In addition to macrophages, the induction of receptor expression was also observed in other cells and the two receptors showed different patterns. The IL-4R was most intense in endothelial cells in addition to macrophages, while the IL-10R was most intense in regenerating muscle. The immune system is regulated by cells that produce IL-4 and IL-10 and by cells that respond to IL-4 or IL-10. We are only at the beginning of learning how cytokine/cytokine receptor relationships translate into tissue regeneration. Therefore, it is very important to analyze the interaction of cytokines/cytokine receptors using protein-protein interactions. Cytokine/receptor PLA results demonstrated that IL-4

Preprints (www.preprints.org) | NOT PEER-REVIEWED | Posted: 23 April 2023 doi:10.20944/preprints202304.0741.v1

in particular showed cytokine/receptor interaction around blood vessels and in the epithelial cells. Once the inflammation has subsided, new tissue formation must begin, for which fibroblasts and endothelial cells are essential, along with macrophages [80,81]. Fibroblasts are involved in tissue remodeling and endothelial cells are responsible for the formation of new vascular networks [80,81]. During the wound-healing process, there is continuous communication between macrophages, fibroblasts, and endothelial cells [82]. If there is any failure in the communication needed for tissue regeneration, regeneration fails. This study suggests that endothelial cells are activated simultaneously with macrophages, as simultaneous activation of the IL-4R on the surface of both cells was observed. Furthermore, endothelial cells showed intense IL-4 cytokine/receptor interactions during skin, lung, and muscle regeneration (Figure 11, Table 2). The interaction between IL-13 and IL-4R will be analyzed in the future. This is a cytokine that is also able to bind to IL-4R [20,39]. Different cytokines can induce different pathways and the analysis of both cytokine/receptor interactions could be very important for a better understanding of tissue regeneration.

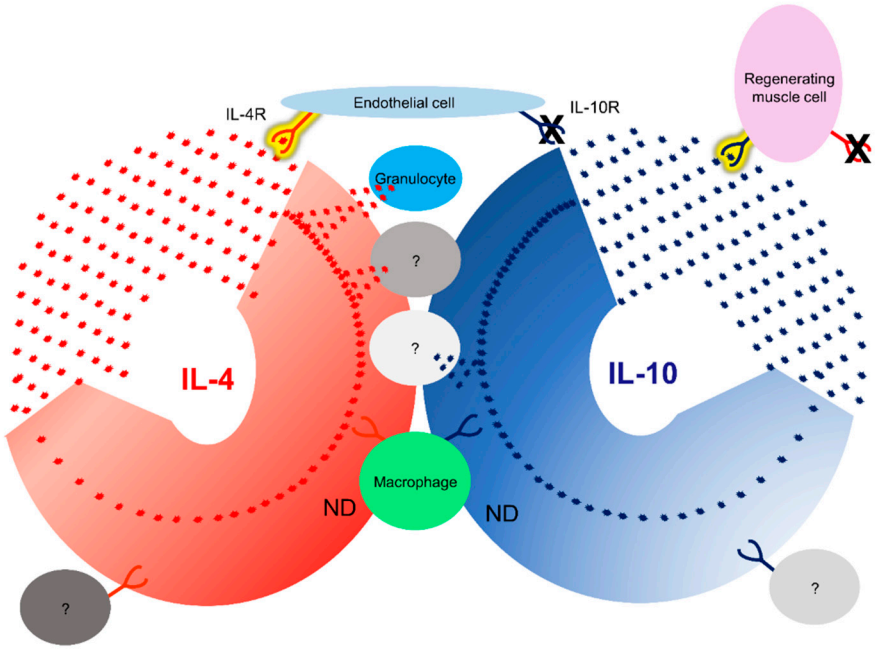

Figure 11. *In situ* identification of both IL-4 and IL-10 cytokine-receptor interactions during tissue regeneration. A schema to resume cytokine, receptor, and interactionswas identified in this study. IL-4 in red, IL-10 in blue. Detected interactions are in yellow.

Using PLA, we have shown that the primary targets of the IL-10 are regenerating muscle cells, contrary to the activation observed for IL-4. In the skin and lungs, IL-10 activation was very low whereas, a very high level of activation was observed in regenerating muscle cells.

5. Conclusions

In summary, we can conclude that:

1. Using immunolabeling, M2-like macrophages were identified in regenerating tissues.
2. Cut-infection-irradiation injuries induced the expression of IL-4 and IL-10 receptors in M2-like macrophages in all three tissues.
3. Cytokine receptor induction was not limited to macrophages, as other cells also showed receptor induction.

Preprints (www.preprints.org) | NOT PEER-REVIEWED | Posted: 23 April 2023 doi:10.20944/preprints202304.0741.v1

4. The two different cytokine receptors showed different localization. IL-4R expression was mainly expressed in endothelial cells and localized around the vasculature. IL-10R expression was particularly intense in the regenerating irradiated muscle cells.

5. The PLA method provided valuable information for a better understanding of tissue regeneration. Using this technique, we have shown that IL-4 can interact with its receptor around the vasculature and IL-10 interacts with its receptor in regenerating muscle.

6. Granulocytes do not have an IL-4 cytokine/receptor interaction, suggesting that these cells are not targest but are a source of cytokine.

These results validate that the strategy implemented to detect those interactions *in situ* is functional.

Table 2. Cytokine-receptor interaction for both IL-4 and IL-10 was identified in situ. (A) expression and (B) interaction during tissue regeneration. IL-4 in red, IL-10 in blue. *: was not identified in muscle tissue, because only a few granulocytes could be detected; ND: not determined.

A

Expression	**IL-4**		**IL-10**	
Skin/lung/muscle	**Cytokine**	Receptor	Cytokine	Receptor
Granulocyte	+*	-	-	-
Macrophage	ND	+	ND	+
Endothelial cell	-	+	-	-
Regenerating muscle cell	-	-	-	+
Uncharacterized cell	+	+	-	-
Uncharacterized cell	-	-	+	+

B

Cytokine/Receptor Interaction	**IL-4/IL-4R**	**IL-10/IL-10R**
Endothelial cell	+	-
Regenerating muscle cell	-	+

Supplementary Materials: The following supporting information can be downloaded at: www.mdpi.com/xxx/s1, Figure S1. Identification of IL-4R+ and CD206+ cells *in situ*. (A,B) Immunolabeling with anti-IL-4R and anti-CD206 antibodies of the skin, (C,D) the muscle, and (E,F) the lung sections. (A,C,E) Healthy-tissue. (B,D,F) Wounded-tissue. (A) Negative control of Figure 5A; (B) Negative control of Figure 5B; (C) Negative control of Figure 5E; (D) Negative control of Figure 5F; (E) Negative control of Figure 5I; (F) Negative control of Figure 5J,K. Anti-IL-4R (Alexa488, green fluorescence) and Anti-CD206 (Alexa568, red fluorescence) labeling the M2-like macrophages. Nuclear staining with DAPI (blue fluorescence). Scale bar = 50 µm. Figure S2. Identification of IL-10R+ and CD206+ cells *in situ*. (A,B) Immunolabeling of both anti-IL-10R and anti-CD206 antibodies of the skin, (C,D) the lung, and (E,F) the muscle sections. (A,C,E) Healthy-tissue. (B,D,F) Wounded-tissue. (A) Negative control of Figure 6A; (B) Negative control of Figure 6B; (C) Negative control of Figure 6E; (D) Negative control of Figure 6F; (E) Negative control of Figure 6I; (F) Negative control of Figure 6J-L. Anti-IL-10R (Alexa488, green fluorescence) and Anti-CD206 (Alexa568, red fluorescence) labeling the tissue-resident and M2-like macrophages. Nuclear staining with DAPI (blue fluorescence). Scale bar = 50 µm. Figure S3. Identification of IL-4R+ and IL-4+ cells *in situ*. (A,B) Immunolabeling of both anti-IL-4R and IL-4 antibodies in the healthy skin, (C,D) the lung, and (E,F) the muscle sections. (B,D,F) Expanded view: high magnification image of the area within the red rectangle in A,C,E. Anti-IL-4R (Alexa488, green fluorescence) and Anti-IL-4 (Alexa568, red fluorescence). Nuclear staining with DAPI (blue fluorescence). Scale bar = 20 µm. Arrowhead: IL-4R+ cells. Figure S4. Identification of IL-4R+ and IL-4+ cells *in situ*. (A,B) Immunolabeling of both anti-IL-4R and IL-4 antibodies in the skin, (C,D) the lung, and (E,F) the muscle sections. (A,C,E) Healthy-tissue. (B,D,F) Wounded-tissue. (A) Negative control of Figure S3A,B; (B) Negative control of Figure 7A,B; (C) Negative control of Figure S3C,D; (D) Negative control of Figure 7C,D; (E) Negative control of Figure S3E,F; (F) Negative control

of Figure 7E,F. Anti-IL-4R (Alexa488, green fluorescence) and Anti-IL-4 (Alexa568, red fluorescence). Nuclear staining with DAPI (blue fluorescence). Scale bar = 20 μm. Figure S5. Identification of IL-10R+ and IL-10+ cells *in situ*. (A,B) Immunolabeling of both anti-IL-10R and IL-10 antibodies in the healthy skin, (C,D) the lun,g and (E,F) the muscle sections. (B,D,F) Expanded view: high magnification image of the area within the red rectangle in A,C,E. Anti-IL-10R (Alexa488, green fluorescence) and Anti-IL-10 (Alexa568, red fluorescence). Nuclear staining with DAPI (blue fluorescence). Scale bar = 20 μm. Thin arrow: IL-10R+ cell. Figure S6. Identification of IL-10R+ and IL-10+ cells *in situ*. (A,B) Immunolabeling with anti-IL-10R and IL-10 antibodies in the skin, (C,D) the lun,g and (E,F) the muscle sections. (A,C,E) Healthy-tissue. (B,D,F) Wounded-tissue. (A) Negative control of Figure S5A,B; (B) Negative control of Figure 8A,B; (C) Negative control of Figure S5C,D; (D) Negative control of Figure 8C,D; (E) Negative control of Figure S5E,F; (F) Negative control of Figure 8E,F. Anti-IL-10R (Alexa488, green fluorescence) and Anti-IL-10 (Alexa568, red fluorescence). Nuclear staining with DAPI (blue fluorescence). Scale bar = 20 μm. Figure S7. Interaction between IL-4 and IL-4 IL-4R *in situ*. (A,B) Proximity Ligation Assay with anti-IL-4R and anti-IL-4 antibodies in the healthy skin, (C,D) the healthy lun,g and (E,F) the healthy muscle. (B,D,F) Expanded view: high magnification image of the area within the red rectangle in A,C,E. Alexa568, yellow fluorescence, labeling the interaction between IL-4 and IL-4R. Nuclear staining with DAPI (blue fluorescence). Scale bar = 20 μm. Arrow: Proximity Ligation Assay IL-4R/IL-4 positive cells. Figure S8. Interaction between IL-10 and IL-10R *in situ*. (A,B) Proximity Ligation Assay with anti-IL-10R and anti-IL-10 in the healthy skin, (C,D) the healthy lun,g and (E,F) the healthy muscle. (B,D,F) Expanded view: high magnification image of the area within the red rectangle in A,C,E. Alexa568, yellow fluorescence, labeling the interaction between IL-10 and IL-10R. Nuclear staining with DAPI (blue fluorescence). Scale bar = 20 μm. Arrow: Proximity Ligation Assay IL-10R+/IL-10+ cells. Figure S9. Interaction between IL-4/IL-4R and IL-10/IL-10R *in situ*. (A,B) Proximity Ligation Assay with anti-IL-4 and anti-IL-4R; anti-IL-10 and anti-IL-10R antibodies in the skin, (C,D) the lun,g and (E,F) the muscle sections. (A,C,E) Healthy-tissue. (B,D,F) Wounded-tissue. (A) Negative control of Figure S7A,B and S8A,B; (B) Negative control of Figure 9A,B and 10A,B; (C) Negative control of Figure S7C,D and S8C,D; (D) Negative control of Figure 9C,D and 10C,D; (E) Negative control of Figure S7E,F and S8E,F; (F) Negative control of Figure 9E,F and 10E,F. Alexa568, yellow fluorescence, labeling the interaction between IL-4 and IL-4R; IL-10 and IL-10R. Nuclear staining with DAPI (blue fluorescence). Scale bar = 20 μm.

Author Contributions: K.N., A.-L.F., and D.R. designed the experiments; C.M., M.R. and J.G. performed the immunofluorescence and PLA. K.N., A.-L.F,. and D.R., designed the analytical approaches; F. D-G. provided skin and lung samples; D.R. provided muscle samples. K.N., A.-L.F., and D.R. wrote the manuscript with input from all the authors. All authors discussed the results. All authors have read and agreed to the published version of the manuscript.

Funding: This research was funded by the Délégation Générale de l'Armement (DGA), grant number (PDH2-NRBC-4-NR-4306) and (PDH-SAN-1-227).

Institutional Review Board Statement: This study was approved by the French Army Animal Ethics Committee (N°2011/22.1). All pigs were treated in compliance with the European legislation (dir 2010/63/EU) implemented into French law (decree 2013-118) regulating animal experimentation.

Acknowledgments: We are very grateful to Robert Drillien for his helpful advice and critical reviewingof our manuscript. We are very grateful to Nathalie Guatto and Xavier Butigieg for their helpful advice and sample and image preparations. Work was supported by the Delegation Générale de l'Armement (DGA) (PDH2-NRBC-4-NR-4306 and PDH-SAN-1-217/206).

Conflicts of Interest: The authors declare no conflict of interest.

References

1. Martinez, F.O.; Gordon, S. The M1 and M2 Paradigm of Macrophage Activation: Time for Reassessment. F1000Prime Rep 2014, 6, 13, doi:10.12703/P6-13.
2. Snyder, R.J.; Lantis, J.; Kirsner, R.S.; Shah, V.; Molyneaux, M.; Carter, M.J. Macrophages: A Review of Their Role in Wound Healing and Their Therapeutic Use. Wound Repair Regen 2016, 24, 613–629, doi:10.1111/wrr.12444.
3. Abdelaziz, M.H.; Abdelwahab, S.F.; Wan, J.; Cai, W.; Huixuan, W.; Jianjun, C.; Kumar, K.D.; Vasudevan, A.; Sadek, A.; Su, Z.; et al. Alternatively Activated Macrophages; a Double-Edged Sword in Allergic Asthma. J Transl Med 2020, 18, 58, doi:10.1186/s12967-020-02251-w.
4. Xu, H.-T.; Lee, C.-W.; Li, M.-Y.; Wang, Y.-F.; Yung, P.S.-H.; Lee, O.K.-S. The Shift in Macrophages Polarisation after Tendon Injury: A Systematic Review. J Orthop Translat 2020, 21, 24–34, doi:10.1016/j.jot.2019.11.009.
5. Arora, S.; Dev, K.; Agarwal, B.; Das, P.; Syed, M.A. Macrophages: Their Role, Activation, and Polarization in Pulmonary Diseases. Immunobiology 2018, 223, 383–396, doi:10.1016/j.imbio.2017.11.001.

6. Shapouri-Moghaddam, A.; Mohammadian, S.; Vazini, H.; Taghadosi, M.; Esmaeili, S.-A.; Mardani, F.; Seifi, B.; Mohammadi, A.; Afshari, J.T.; Sahebkar, A. Macrophage Plasticity, Polarization, and Function in Health and Disease. J Cell Physiol 2018, 233, 6425–6440, doi:10.1002/jcp.26429.
7. Gharib, S.A.; McMahan, R.S.; Eddy, W.E.; Long, M.E.; Parks, W.C.; Aitken, M.L.; Manicone, A.M. Transcriptional and Functional Diversity of Human Macrophage Repolarization. J Allergy Clin Immunol 2019, 143, 1536–1548, doi:10.1016/j.jaci.2018.10.046.
8. Tidball, J.G.; Dorshkind, K.; Wehling-Henricks, M. Shared Signaling Systems in Myeloid Cell-Mediated Muscle Regeneration. Development 2014, 141, 1184–1196, doi:10.1242/dev.098285.
9. Kieler, M.; Hofmann, M.; Schabbauer, G. More than Just Protein Building Blocks: How Amino Acids and Related Metabolic Pathways Fuel Macrophage Polarization. FEBS J 2021, 288, 3694–3714, doi:10.1111/febs.15715.
10. Hoeksema, M.A.; Shen, Z.; Holtman, I.R.; Zheng, A.; Spann, N.J.; Cobo, I.; Gymrek, M.; Glass, C.K. Mechanisms Underlying Divergent Responses of Genetically Distinct Macrophages to IL-4. Sci Adv 2021, 7, doi:10.1126/sciadv.abf9808.
11. Howard, M.; Farrar, J.; Hilfiker, M.; Johnson, B.; Takatsu, K.; Hamaoka, T.; Paul, W.E. Identification of a T Cell-Derived b Cell Growth Factor Distinct from Interleukin 2. J Exp Med 1982, 155, 914–923, doi:10.1084/jem.155.3.914.
12. Isakson, P.C.; Puré, E.; Vitetta, E.S.; Krammer, P.H. T Cell-Derived B Cell Differentiation Factor(s). Effect on the Isotype Switch of Murine B Cells. J Exp Med 1982, 155, 734–748, doi:10.1084/jem.155.3.734.
13. Mosmann, T.R.; Cherwinski, H.; Bond, M.W.; Giedlin, M.A.; Coffman, R.L. Two Types of Murine Helper T Cell Clone. I. Definition According to Profiles of Lymphokine Activities and Secreted Proteins. J Immunol 1986, 136, 2348–2357.
14. Brown, A.M. A Spreadsheet Template Compatible with Microsoft Excel and IWork Numbers That Returns the Simultaneous Confidence Intervals for All Pairwise Differences between Multiple Sample Means. Computer Methods and Programs in Biomedicine 2010, 98, 76–82, doi:10.1016/j.cmpb.2009.10.001.
15. Yoshimoto, T.; Bendelac, A.; Watson, C.; Hu-Li, J.; Paul, W.E. Role of NK1.1+ T Cells in a TH2 Response and in Immunoglobulin E Production. Science 1995, 270, 1845–1847, doi:10.1126/science.270.5243.1845.
16. Nonaka, M.; Nonaka, R.; Woolley, K.; Adelroth, E.; Miura, K.; Okhawara, Y.; Glibetic, M.; Nakano, K.; O'Byrne, P.; Dolovich, J. Distinct Immunohistochemical Localization of IL-4 in Human Inflamed Airway Tissues. IL-4 Is Localized to Eosinophils in Vivo and Is Released by Peripheral Blood Eosinophils. J Immunol 1995, 155, 3234–3244.
17. Moro, K.; Yamada, T.; Tanabe, M.; Takeuchi, T.; Ikawa, T.; Kawamoto, H.; Furusawa, J.-I.; Ohtani, M.; Fujii, H.; Koyasu, S. Innate Production of T(H)2 Cytokines by Adipose Tissue-Associated c-Kit(+)Sca-1(+) Lymphoid Cells. Nature 2010, 463, 540–544, doi:10.1038/nature08636.
18. Saenz, S.A.; Siracusa, M.C.; Perrigoue, J.G.; Spencer, S.P.; Urban, J.F.J.; Tocker, J.E.; Budelsky, A.L.; Kleinschek, M.A.; Kastelein, R.A.; Kambayashi, T.; et al. IL25 Elicits a Multipotent Progenitor Cell Population That Promotes T(H)2 Cytokine Responses. Nature 2010, 464, 1362–1366, doi:10.1038/nature08901.
19. Paul, W.E. History of Interleukin-4. Cytokine 2015, 75, 3–7, doi:10.1016/j.cyto.2015.01.038.
20. Junttila, I.S. Tuning the Cytokine Responses: An Update on Interleukin (IL)-4 and IL-13 Receptor Complexes. Front Immunol 2018, 9, 888, doi:10.3389/fimmu.2018.00888.
21. Iwaszko, M.; Biały, S.; Bogunia-Kubik, K. Significance of Interleukin (IL)-4 and IL-13 in Inflammatory Arthritis. Cells 2021, 10, doi:10.3390/cells10113000.
22. Song, X.; Traub, B.; Shi, J.; Kornmann, M. Possible Roles of Interleukin-4 and -13 and Their Receptors in Gastric and Colon Cancer. Int J Mol Sci 2021, 22, doi:10.3390/ijms22020727.
23. Fiorentino, D.F.; Bond, M.W.; Mosmann, T.R. Two Types of Mouse T Helper Cell. IV. Th2 Clones Secrete a Factor That Inhibits Cytokine Production by Th1 Clones. J Exp Med 1989, 170, 2081–2095, doi:10.1084/jem.170.6.2081.
24. Yssel, H.; De Waal Malefyt, R.; Roncarolo, M.G.; Abrams, J.S.; Lahesmaa, R.; Spits, H.; de Vries, J.E. IL-10 Is Produced by Subsets of Human CD4+ T Cell Clones and Peripheral Blood T Cells. J Immunol 1992, 149, 2378–2384.
25. Moore, K.W.; de Waal Malefyt, R.; Coffman, R.L.; O'Garra, A. Interleukin-10 and the Interleukin-10 Receptor. Annu Rev Immunol 2001, 19, 683–765, doi:10.1146/annurev.immunol.19.1.683.
26. Nguyen, T.-V.V.; Frye, J.B.; Zbesko, J.C.; Stepanovic, K.; Hayes, M.; Urzua, A.; Serrano, G.; Beach, T.G.; Doyle, K.P. Multiplex Immunoassay Characterization and Species Comparison of Inflammation in Acute and Non-Acute Ischemic Infarcts in Human and Mouse Brain Tissue. acta neuropathol commun 2016, 4, 100, doi:10.1186/s40478-016-0371-y.
27. Kucuksezer, U.C.; Aktas Cetin, E.; Esen, F.; Tahrali, I.; Akdeniz, N.; Gelmez, M.Y.; Deniz, G. The Role of Natural Killer Cells in Autoimmune Diseases. Front Immunol 2021, 12, 622306, doi:10.3389/fimmu.2021.622306.

28. Nagata, K.; Nishiyama, C. IL-10 in Mast Cell-Mediated Immune Responses: Anti-Inflammatory and Proinflammatory Roles. Int J Mol Sci 2021, 22, doi:10.3390/ijms22094972.
29. Jarry, A.; Bossard, C.; Bou-Hanna, C.; Masson, D.; Espaze, E.; Denis, M.G.; Laboisse, C.L. Mucosal IL-10 and TGF-Beta Play Crucial Roles in Preventing LPS-Driven, IFN-Gamma-Mediated Epithelial Damage in Human Colon Explants. J Clin Invest 2008, 118, 1132–1142, doi:10.1172/JCI32140.
30. Saraiva, M.; Vieira, P.; O'Garra, A. Biology and Therapeutic Potential of Interleukin-10. J Exp Med 2020, 217, doi:10.1084/jem.20190418.
31. Howes, A.; Taubert, C.; Blankley, S.; Spink, N.; Wu, X.; Graham, C.M.; Zhao, J.; Saraiva, M.; Ricciardi-Castagnoli, P.; Bancroft, G.J.; et al. Differential Production of Type I IFN Determines the Reciprocal Levels of IL-10 and Proinflammatory Cytokines Produced by C57BL/6 and BALB/c Macrophages. J Immunol 2016, 197, 2838–2853, doi:10.4049/jimmunol.1501923.
32. Frangogiannis, N.G. Regulation of the Inflammatory Response in Cardiac Repair. Circ Res 2012, 110, 159–173, doi:10.1161/CIRCRESAHA.111.243162.
33. Davies, L.C.; Jenkins, S.J.; Allen, J.E.; Taylor, P.R. Tissue-Resident Macrophages. Nat Immunol 2013, 14, 986–995, doi:10.1038/ni.2705.
34. Hashimoto, I.; Imaizumi, K.; Hashimoto, N.; Furukawa, H.; Noda, Y.; Kawabe, T.; Honda, T.; Ogawa, T.; Matsuo, M.; Imai, N.; et al. Aqueous Fraction of Sauropus Androgynus Might Be Responsible for Bronchiolitis Obliterans. Respirology 2013, 18, 340–347, doi:10.1111/j.1440-1843.2012.02286.x.
35. Qian, B.-Z.; Pollard, J.W. Macrophage Diversity Enhances Tumor Progression and Metastasis. Cell 2010, 141, 39–51, doi:10.1016/j.cell.2010.03.014.
36. Stein, M.; Keshav, S.; Harris, N.; Gordon, S. Interleukin 4 Potently Enhances Murine Macrophage Mannose Receptor Activity: A Marker of Alternative Immunologic Macrophage Activation. J Exp Med 1992, 176, 287–292, doi:10.1084/jem.176.1.287.
37. Gordon, S. Alternative Activation of Macrophages. Nat Rev Immunol 2003, 3, 23–35, doi:10.1038/nri978.
38. Gordon, S.; Lawson, L.; Rabinowitz, S.; Crocker, P.R.; Morris, L.; Perry, V.H. Antigen Markers of Macrophage Differentiation in Murine Tissues. Curr Top Microbiol Immunol 1992, 181, 1–37, doi:10.1007/978-3-642-77377-8_1.
39. McKenzie, G.J.; Bancroft, A.; Grencis, R.K.; McKenzie, A.N. A Distinct Role for Interleukin-13 in Th2-Cell-Mediated Immune Responses. Curr Biol 1998, 8, 339–342, doi:10.1016/s0960-9822(98)70134-4.
40. Sica, A.; Mantovani, A. Macrophage Plasticity and Polarization: In Vivo Veritas. J Clin Invest 2012, 122, 787–795, doi:10.1172/JCI59643.
41. Martinez, F.O.; Sica, A.; Mantovani, A.; Locati, M. Macrophage Activation and Polarization. Front Biosci 2008, 13, 453–461, doi:10.2741/2692.
42. Nikovics, K.; Favier, A.-L. Macrophage Identification In Situ. Biomedicines 2021, 9, doi:10.3390/biomedicines9101393.
43. Wynn, T.A.; Chawla, A.; Pollard, J.W. Macrophage Biology in Development, Homeostasis and Disease. Nature 2013, 496, 445–455, doi:10.1038/nature12034.
44. Wang, L.-X.; Zhang, S.-X.; Wu, H.-J.; Rong, X.-L.; Guo, J. M2b Macrophage Polarization and Its Roles in Diseases. J Leukoc Biol 2019, 106, 345–358, doi:10.1002/JLB.3RU1018-378RR.
45. Lin, J.-S.; Lai, E.-M. Protein-Protein Interactions: Yeast Two-Hybrid System. Methods Mol Biol 2017, 1615, 177–187, doi:10.1007/978-1-4939-7033-9_14.
46. Wang, Y.; Wang, N. FRET and Mechanobiology. Integr Biol (Camb) 2009, 1, 565–573, doi:10.1039/b913093b.
47. Miller, K.E.; Kim, Y.; Huh, W.-K.; Park, H.-O. Bimolecular Fluorescence Complementation (BiFC) Analysis: Advances and Recent Applications for Genome-Wide Interaction Studies. J Mol Biol 2015, 427, 2039–2055, doi:10.1016/j.jmb.2015.03.005.
48. Fredriksson, S.; Gullberg, M.; Jarvius, J.; Olsson, C.; Pietras, K.; Gústafsdóttir, S.M.; Ostman, A.; Landegren, U. Protein Detection Using Proximity-Dependent DNA Ligation Assays. Nat Biotechnol 2002, 20, 473–477, doi:10.1038/nbt0502-473.
49. Gullberg, M.; Gústafsdóttir, S.M.; Schallmeiner, E.; Jarvius, J.; Bjarnegård, M.; Betsholtz, C.; Landegren, U.; Fredriksson, S. Cytokine Detection by Antibody-Based Proximity Ligation. Proc Natl Acad Sci U S A 2004, 101, 8420–8424, doi:10.1073/pnas.0400552101.
50. Bagchi, S.; Fredriksson, R.; Wallén-Mackenzie, Å. In Situ Proximity Ligation Assay (PLA). Methods Mol Biol 2015, 1318, 149–159, doi:10.1007/978-1-4939-2742-5_15.
51. Alam, M.S. Proximity Ligation Assay (PLA). Curr Protoc Immunol 2018, 123, e58, doi:10.1002/cpim.58.
52. Wang, P.; Yang, Y.; Hong, T.; Zhu, G. Proximity Ligation Assay: An Ultrasensitive Method for Protein Quantification and Its Applications in Pathogen Detection. Appl Microbiol Biotechnol 2021, 105, 923–935, doi:10.1007/s00253-020-11049-1.
53. Ezzelarab, M.B.; Cooper, D.K.C. Systemic Inflammation in Xenograft Recipients (SIXR): A New Paradigm in Pig-to-Primate Xenotransplantation? Int J Surg 2015, 23, 301–305, doi:10.1016/j.ijsu.2015.07.643.
54. Lunney, J.K.; Van Goor, A.; Walker, K.E.; Hailstock, T.; Franklin, J.; Dai, C. Importance of the Pig as a Human Biomedical Model. Sci Transl Med 2021, 13, eabd5758, doi:10.1126/scitranslmed.abd5758.

55. Sullivan, T.P.; Eaglstein, W.H.; Davis, S.C.; Mertz, P. The Pig as a Model for Human Wound Healing. Wound Repair Regen 2001, 9, 66–76, doi:10.1046/j.1524-475x.2001.00066.x.
56. Riccobono, D.; Nikovics, K.; François, S.; Favier, A.-L.; Jullien, N.; Schrock, G.; Scherthan, H.; Drouet, M. First Insights Into the M2 Inflammatory Response After Adipose-Tissue-Derived Stem Cell Injections in Radiation-Injured Muscles. Health Physics 2018, 115, 37–48, doi:10.1097/HP.0000000000000822.
57. Nikovics, K.; Durand, M.; Castellarin, C.; Burger, J.; Sicherre, E.; Collombet, J.-M.; Oger, M.; Holy, X.; Favier, A.-L. Macrophages Characterization in an Injured Bone Tissue. Biomedicines 2022, 10, doi:10.3390/biomedicines10061385.
58. Midway, S.; Robertson, M.; Flinn, S.; Kaller, M. Comparing Multiple Comparisons: Practical Guidance for Choosing the Best Multiple Comparisons Test. PeerJ 2020, 8, e10387, doi:10.7717/peerj.10387.
59. Xu, J.; Yu, L.; Guo, J.; Xiang, J.; Zheng, Z.; Gao, D.; Shi, B.; Hao, H.; Jiao, D.; Zhong, L.; et al. Generation of Pig Induced Pluripotent Stem Cells Using an Extended Pluripotent Stem Cell Culture System. Stem Cell Res Ther 2019, 10, 193, doi:10.1186/s13287-019-1303-0.
60. Minutti, C.M.; Knipper, J.A.; Allen, J.E.; Zaiss, D.M.W. Tissue-Specific Contribution of Macrophages to Wound Healing. Semin Cell Dev Biol 2017, 61, 3–11, doi:10.1016/j.semcdb.2016.08.006.
61. Pan, D.; Schellhardt, L.; Acevedo-Cintron, J.A.; Hunter, D.; Snyder-Warwick, A.K.; Mackinnon, S.E.; Wood, M.D. IL-4 Expressing Cells Are Recruited to Nerve after Injury and Promote Regeneration. Exp Neurol 2022, 347, 113909, doi:10.1016/j.expneurol.2021.113909.
62. Orecchioni, M.; Ghosheh, Y.; Pramod, A.B.; Ley, K. Macrophage Polarization: Different Gene Signatures in M1(LPS+) vs. Classically and M2(LPS-) vs. Alternatively Activated Macrophages. Front Immunol 2019, 10, 1084, doi:10.3389/fimmu.2019.01084.
63. Zizzo, G.; Hilliard, B.A.; Monestier, M.; Cohen, P.L. Efficient Clearance of Early Apoptotic Cells by Human Macrophages Requires M2c Polarization and MerTK Induction. J Immunol 2012, 189, 3508–3520, doi:10.4049/jimmunol.1200662.
64. Xu, W.; Zhao, X.; Daha, M.R.; van Kooten, C. Reversible Differentiation of Pro- and Anti-Inflammatory Macrophages. Mol Immunol 2013, 53, 179–186, doi:10.1016/j.molimm.2012.07.005.
65. Arnold, D.E.; Heimall, J.R. A Review of Chronic Granulomatous Disease. Adv Ther 2017, 34, 2543–2557, doi:10.1007/s12325-017-0636-2.
66. Jenkins, S.J.; Ruckerl, D.; Thomas, G.D.; Hewitson, J.P.; Duncan, S.; Brombacher, F.; Maizels, R.M.; Hume, D.A.; Allen, J.E. IL-4 Directly Signals Tissue-Resident Macrophages to Proliferate beyond Homeostatic Levels Controlled by CSF-1. J Exp Med 2013, 210, 2477–2491, doi:10.1084/jem.20121999.
67. Shintani, Y.; Ito, T.; Fields, L.; Shiraishi, M.; Ichihara, Y.; Sato, N.; Podaru, M.; Kainuma, S.; Tanaka, H.; Suzuki, K. IL-4 as a Repurposed Biological Drug for Myocardial Infarction through Augmentation of Reparative Cardiac Macrophages: Proof-of-Concept Data in Mice. Sci Rep 2017, 7, 6877, doi:10.1038/s41598-017-07328-z.
68. Huynh, T.; Reed, C.; Blackwell, Z.; Phelps, P.; Herrera, L.C.P.; Almodovar, J.; Zaharoff, D.A.; Wolchok, J. Local IL-10 Delivery Modulates the Immune Response and Enhances Repair of Volumetric Muscle Loss Muscle Injury. Sci Rep 2023, 13, 1983, doi:10.1038/s41598-023-27981-x.
69. de Waal Malefyt, R.; Abrams, J.; Bennett, B.; Figdor, C.G.; de Vries, J.E. Interleukin 10(IL-10) Inhibits Cytokine Synthesis by Human Monocytes: An Autoregulatory Role of IL-10 Produced by Monocytes. J Exp Med 1991, 174, 1209–1220, doi:10.1084/jem.174.5.1209.
70. O'Farrell, A.M.; Liu, Y.; Moore, K.W.; Mui, A.L. IL-10 Inhibits Macrophage Activation and Proliferation by Distinct Signaling Mechanisms: Evidence for Stat3-Dependent and -Independent Pathways. EMBO J 1998, 17, 1006–1018, doi:10.1093/emboj/17.4.1006.
71. Dagdeviren, S.; Jung, D.Y.; Lee, E.; Friedline, R.H.; Noh, H.L.; Kim, J.H.; Patel, P.R.; Tsitsilianos, N.; Tsitsilianos, A.V.; Tran, D.A.; et al. Altered Interleukin-10 Signaling in Skeletal Muscle Regulates Obesity-Mediated Inflammation and Insulin Resistance. Mol Cell Biol 2016, 36, 2956–2966, doi:10.1128/MCB.00181-16.
72. Sun, S.-J.; Wei, R.; Li, F.; Liao, S.-Y.; Tse, H.-F. Mesenchymal Stromal Cell-Derived Exosomes in Cardiac Regeneration and Repair. Stem Cell Reports 2021, 16, 1662–1673, doi:10.1016/j.stemcr.2021.05.003.
73. Jorda, A.; Campos-Campos, J.; Aldasoro, C.; Colmena, C.; Aldasoro, M.; Alvarez, K.; Valles, S.L. Protective Action of Ultrasound-Guided Electrolysis Technique on the Muscle Damage Induced by Notexin in Rats. PLoS One 2022, 17, e0276634, doi:10.1371/journal.pone.0276634.
74. Hong, E.-G.; Ko, H.J.; Cho, Y.-R.; Kim, H.-J.; Ma, Z.; Yu, T.Y.; Friedline, R.H.; Kurt-Jones, E.; Finberg, R.; Fischer, M.A.; et al. Interleukin-10 Prevents Diet-Induced Insulin Resistance by Attenuating Macrophage and Cytokine Response in Skeletal Muscle. Diabetes 2009, 58, 2525–2535, doi:10.2337/db08-1261.
75. Chang, C.-M.; Lam, H.Y.P.; Hsu, H.-J.; Jiang, S.-J. Interleukin-10: A Double-Edged Sword in Breast Cancer. Tzu Chi Med J 2021, 33, 203–211, doi:10.4103/tcmj.tcmj_162_20.
76. Silk, A.W.; Margolin, K. Cytokine Therapy. Hematol Oncol Clin North Am 2019, 33, 261–274, doi:10.1016/j.hoc.2018.12.004.

77. Ho, I.-C.; Miaw, S.-C. Regulation of IL-4 Expression in Immunity and Diseases. Adv Exp Med Biol 2016, 941, 31–77, doi:10.1007/978-94-024-0921-5_3.
78. Ohara, J.; Paul, W.E. Receptors for B-Cell Stimulatory Factor-1 Expressed on Cells of Haematopoietic Lineage. Nature 1987, 325, 537–540, doi:10.1038/325537a0.
79. von Haehling, S.; Wolk, K.; Höflich, C.; Kunz, S.; Grünberg, B.H.; Döcke, W.-D.; Reineke, U.; Asadullah, K.; Sterry, W.; Volk, H.-D.; et al. Interleukin-10 Receptor-1 Expression in Monocyte-Derived Antigen-Presenting Cell Populations: Dendritic Cells Partially Escape from IL-10's Inhibitory Mechanisms. Genes Immun 2015, 16, 8–14, doi:10.1038/gene.2014.69.
80. Moretti, L.; Stalfort, J.; Barker, T.H.; Abebayehu, D. The Interplay of Fibroblasts, the Extracellular Matrix, and Inflammation in Scar Formation. J Biol Chem 2022, 298, 101530, doi:10.1016/j.jbc.2021.101530.
81. Li, S.; Ding, X.; Zhang, H.; Ding, Y.; Tan, Q. IL-25 Improves Diabetic Wound Healing through Stimulating M2 Macrophage Polarization and Fibroblast Activation. Int Immunopharmacol 2022, 106, 108605, doi:10.1016/j.intimp.2022.108605.
82. Ronca, R.; Van Ginderachter, J.A.; Turtoi, A. Paracrine Interactions of Cancer-Associated Fibroblasts, Macrophages and Endothelial Cells: Tumor Allies and Foes. Curr Opin Oncol 2018, 30, 45–53, doi:10.1097/CCO.0000000000000420.